

1 **Targeted genotyping-by-sequencing of potato and software for imputation**

2

3 Jeffrey B. Endelman^{*1}, Moctar Kante², Hannele Lindqvist-Kreuze², Andrzej Kilian³, Laura M.
4 Shannon⁴, Maria V. Caraza-Harter¹, Brieanne Vaillancourt⁵, Kathrine Mailloux⁵, John P.
5 Hamilton⁵, C. Robin Buell⁵

6

7 ¹Department of Plant & Agroecosystem Sciences, University of Wisconsin–Madison, Madison,
8 WI, USA.

9 ²Genomics, Genetics and Crop Improvement, International Potato Center, Lima, Peru.

10 ³Diversity Arrays Technology Pty Ltd, University of Canberra, Bruce, ACT, Australia.

11 ⁴Department of Horticultural Science, University of Minnesota, Saint Paul, MN, USA.

12 ⁵Center for Applied Genetic Technologies, University of Georgia, Athens, GA, USA

13

14 *Corresponding author (endelman@wisc.edu)

15

16 J.B.E. ORCID 0000-0003-0957-4337

17 M.K. ORCID 0000-0003-4669-3132

18 H.L-K. ORCID 0000-0002-6523-8824

19 L.M.S. ORCID 0000-0003-3935-4909

20 M.C-H. ORCID 0000-0002-5934-1526

21 B.V. ORCID 0000-0002-6795-5173

22 J.P.H. ORCID 0000-0002-8682-5526

23 C.R.B. ORCID 0000-0002-6727-4677

24 **Core Ideas**

25 1. A mid-density, targeted genotyping-by-sequencing (GBS) assay was developed for potato.

26 2. The GBS assay includes markers for resistance to potato virus Y, golden cyst nematode, and

27 potato wart.

28 3. The GBS assay includes multi-allelic markers for potato maturity and tuber shape.

29 4. The polyBreedR software has functions for manipulating and imputing polyploid marker data

30 in Variant Call Format.

31 5. Linkage Analysis was more accurate than the Random Forest method when imputing from

32 2K to 10K markers.

33 ABSTRACT

34 Mid-density targeted genotyping-by-sequencing (GBS) combines trait-specific markers with
35 thousands of genomic markers at an attractive price for linkage mapping and genomic selection.
36 A 2.5K targeted GBS assay for potato was developed using the DArTagTM technology and later
37 expanded to 4K targets. Genomic markers were selected from the potato InfiniumTM SNP array
38 to maximize genome coverage and polymorphism rates. When sample depth was summarized by
39 marker, the power law $\mu \sim \sigma^{0.8}$ was consistently observed between the mean (μ) and standard
40 deviation (σ). The DArTag and SNP array platforms produced equivalent dendograms in a test
41 set of 298 tetraploid samples, and 83% of the common markers showed good quantitative
42 agreement, with RMSE (root-mean-squared-error) less than 0.5. DArTag is suited for genomic
43 selection candidates in the clonal evaluation trial, coupled with imputation to a higher density
44 platform for the training population. Our hypothesis that linkage analysis would be highly
45 accurate for imputing tetraploid marker data was confirmed: the RMSE was 0.15 compared to
46 0.95 by the Random Forest method in a half-diallel population. Regarding high-value traits, the
47 DArTag markers for resistance to potato virus Y, golden cyst nematode, and potato wart
48 appeared to track their targets successfully, as did multi-allelic markers for maturity and tuber
49 shape. In summary, the potato DArTag assay is a transformative and publicly available
50 technology for potato breeding and genetics.

51 **1 INTRODUCTION**

52 Targeted genotyping-by-sequencing (GBS) has become an essential technology for
53 molecular plant breeding. As with restriction site-associated DNA (RAD) sequencing (Baird et
54 al., 2008; Elshire et al., 2011), targeted GBS is based on sequencing a reduced representation of
55 the genome. A key difference is that targeted GBS uses a fixed set of primer pairs or
56 oligonucleotide baits, with the number of targets designed based on the application and price
57 point (Campbell et al., 2015; Gasc et al., 2016; Ali et al., 2016). DArTag is a targeted GBS
58 method based on PCR with molecular inversion probes (Hardenbol et al. 2003) and scalable to
59 thousands of targets (Hardigan et al., 2023; Zhao et al., 2023). As part of the CGIAR Excellence
60 in Breeding platform, DArTag panels were developed for wheat, maize, rice, cowpea, pigeon
61 pea, common bean, groundnut (peanut), sorghum, and potato (Excellence in Breeding, 2022).
62 This article describes the design and validation of the first potato DArTag panel, which had 2.5K
63 targets, as well as a second design project, which extended the assay to 4K targets.

64 Before DArTag, there was no comparable “mid-density” genotyping service for potato. The
65 main genotyping platform for genetic mapping and genomic selection in potato has been an
66 Infinium™ SNP array, which was originally developed with 8303 markers and then expanded to
67 12K (Version 2) based on the same discovery panel of 6 varieties (Hamilton et al., 2011; Felcher
68 et al., 2012). The 22K V3 array incorporated new SNPs from a larger discovery panel of 83
69 tetraploid varieties (Uitdewilligen et al., 2013; Vos et al., 2015), and the 31K V4 array added
70 markers from yet another discovery pool (Sharma and Bryan, 2017). To maintain backwards
71 compatibility with existing marker data, the genomic markers for DArTag were selected from the
72 potato Infinium array.

73 In addition to genomic markers, the DArTag design includes “essential markers” that are
74 prioritized during the final marker selection and primer design process. For potato, our initial
75 priority was identifying markers with high diagnostic value (i.e., haplotype-specificity) for key
76 resistance genes in a wide variety of genetic backgrounds. When the V1 assay was being
77 designed, in 2020, KASP markers for the *Ry_{adg}* (Herrera et al., 2018) and *Ry_{sto}* (Nie et al., 2016)
78 resistance genes against potato virus Y (PVY) were being widely utilized through a “low-
79 density” genotyping service of the Excellence in Breeding platform. These two markers were
80 therefore obvious candidates to include in the V1 DArTag panel. When the V2 DArTag panel
81 was designed in 2023, a number of additional traits were targeted with essential markers.

82 Our focus for the V1 DArTag assay was tetraploid potato, which is the ploidy level of global
83 commerce. A well-known challenge of GBS in polyploids is the high read depth needed to
84 differentiate heterozygotes with differing allele dosage (Uitdewilligen et al., 2013). The read
85 depth needed to achieve 95% genotyping accuracy in a tetraploid ranges from 30 to 60,
86 depending on the population structure and other assumptions (Gerard et al. 2018; Matias et al.
87 2019). This limitation has motivated the use of pseudo-diploid (aka diploidized) genotype calls
88 in previous studies (Bastien et al., 2018; Matias et al., 2019), but allele dosage information is
89 needed for the partitioning of genetic variance and breeding value prediction in tetraploids
90 (Endelman et al., 2018; de Bem Oliveira et al., 2019). There is little information or software
91 available to facilitate marker imputation in tetraploids, so filling this gap has been one of our
92 research objectives.

93 **2 MATERIALS AND METHODS**

94 **2.1 Genomic markers**

95 SNPs were selected from the 22K V3 SNP array (Felcher et al., 2012; Vos et al., 2015) for
96 the 2.5K V1 DArTag set, and additional SNPs were selected from the V4 31K SNP array for the
97 4K V2 DArTag set. Physical positions were based on the DMv6.1 reference genome (Pham et
98 al., 2020). Genetic map positions (in cM) were interpolated from the map positions reported in
99 Endelman and Jansky (2016). The interpolated “Marey” map of cM vs. bp was constrained to be
100 monotone nondecreasing (Figure S1) using an I-spline basis with 12 degrees of freedom,
101 generated with R/splines2 (Wang and Yan, 2021). Non-negative basis coefficients were
102 computed by minimizing the mean-squared error with R/CVXR (Fu et al., 2020). The script is
103 available as function *interpolate_cM* in R/MapRtools (Endelman, 2023a). Initially, SNPs were
104 selected based on discretizing the genome into 1 cM bins, and within each bin, SNPs were
105 prioritized based on minor allele frequency (MAF) in a collection of US and CIP germplasm.
106 After saturating the genome, additional SNPs were selected sequentially based on the ad-hoc
107 score $d + 10 \times MAF$, where d is cM distance to the closest selected SNP.

108 Germplasm for evaluating V1 DArTag came from the International Potato Center (CIP) and
109 University of Wisconsin breeding programs. Data for 703 tetraploid samples are provided as
110 Supplemental File 1 in Variant Call Format (VCF), with the year of submission (2020, 2021, or
111 2022) for each sample recorded in Supplemental File 2. The function *dart2vcf* in R/polyBreedR
112 (Endelman, 2023b) generates a VCFv4.3 compliant file from the two standard DArTag CSV
113 files (“Allele_Dose_Report” and “Allele_match_counts_collapsed”). R/polyBreedR function *gbs*
114 was used to replace the original DArTag genotype calls (FORMAT field GT) with those based
115 on R/updog, using the “norm” prior (Gerard et al., 2018). Three parameters of the beta-binomial

116 model (SE = sequencing error, AB = allelic bias, OD = overdispersion) were stored for each
117 variant. Both functions utilize R package vcfR (Knaus and Grunwald, 2017).

118 A single submission of tetraploid (N=323) and diploid (N=52) samples was used to evaluate
119 the 4K V2 DArTag assay (Supplemental Files 3 and 4). Genotype calls were made separately for
120 each ploidy group using the *gbs* function in R/polyBreedR.

121 A comparison of DArTag vs. SNP array genotypes was conducted using 298 clones for V1
122 DArTag and 78 clones for V2 DArTag. XY intensity values and genotype calls are provided in
123 Supplemental File 5 for 15,187 markers from the V4 SNP array, based on a normal mixture
124 model estimated with R/fitPoly (Voorrips et al., 2011; Zych et al., 2019). The parameter file for
125 the normal mixture model, which is distributed with R/polyBreedR as
126 “potato_V4array_model.csv”, was used when converting Genome Studio Final Reports to VCF
127 with the function *array2vcf*. This function also requires a VCF map definition file to convert
128 from B allele dosage to ALT dosage, which is distributed as “potato_V4array.vcf” with
129 R/polyBreedR. The common markers between DArTag and the SNP array, including matching
130 REF/ALT, were identified using *bcftools isec* (Danecek et al. 2021).

131

132 **2.2 Imputation**

133 Two methods were compared for the accuracy of imputing SNP array markers from
134 DArTag: Random Forest (RF) and Linkage Analysis (LA). Method RF was implemented as
135 R/polyBreedR function *impute_L2H*, using the R/randomForest package (Liaw and Wiener,
136 2002). The 100 closest markers were used as prediction variables, and the number of trees was
137 set at 100 by monitoring the out-of-bag error. Method LA was implemented as R/polyBreedR
138 function *impute_LA*, using the software PolyOrigin (Zheng et al., 2021). Imputation error was

139 measured using leave-one-family-out cross-validation in a five-parent half-diallel population
140 (pedigree in Supplemental File 6). The parent codes in Table 1 are P1=W6609-3, P2=W12078-
141 76, P3=W13NYP102-7, P4=W14NYQ4-1, P5=W14NYQ9-2. The high density (10K) phased
142 parental genotypes are in Supplemental File 7.

143

144 **2.3 Trait markers**

145 A set of six interconnected F1 populations was used to assess the accuracy of genotype calls
146 for the V2 DArTag trait markers Ryadg_chr11_2499502 and H1_chr05_52349069. Parental
147 phasing and haplotype reconstruction utilized PolyOrigin (Zheng et al., 2021), and binary trait
148 locus (BTL) analysis utilized R/diaQTL (Amadeu et al., 2021). The pedigree, genomic marker,
149 and dominant trait marker files needed for diaQTL are Supplemental Files 8, 9, 10, respectively.
150 Validation of trait marker Sli_chr12_2372490 was based on the Sli_898 KASP marker (Clot et
151 al., 2020; Kaiser et al., 2021).

152 Trait markers CDF1.2_chr05_4488015 and CDF1.4_chr05_4488021 target two different 7
153 bp insertions of *CDF1* (Kloosterman et al., 2013; Gutaker et al., 2019) and contain equivalent
154 information in the DArT MADC (missing allele discovery count) file. The 81-bp haplotypes in
155 the MADC file were aligned using MUSCLE v3.8 (Edgar, 2004). DArTag read counts for CDF1
156 alleles 1, 2, and 4 were tabulated with R/polyBreedR function *madc* and validated against
157 genotypes determined via whole-genome sequencing with NovaSeq 2x150 reads (Song and
158 Endelman, 2023).

159 Genome assemblies of *S. tuberosum* dihaploids were used to validate markers for *OFP20*, a
160 major gene affecting tuber shape (Wu et al. 2018). High molecular weight DNA was extracted
161 from tissue culture plantlets using a CTAB isolation method and Qiagen Genomic tips (Hilden,

162 Germany), followed by an Amicon filter (MilliporeSigma, Burlington, MA) buffer exchange
163 (Vaillancourt et al., 2019) or Takara NucleoBond HMW DNA kit (Takara, Kusatsu, Shiga,
164 Japan). Genome assembly used hifiasm v0.16.1-r375 (Cheng et al. 2021, 2022) with PacBio HiFi
165 Sequel II (Menlo Park, CA) reads from the University of Minnesota Genomics Center. Contigs
166 less than 50kb were discarded using seqkit v2.3.0 (Shen et al. 2016), followed by Ragtag v2.1.0
167 (Alonge et al. 2019) to scaffold with DM 1-3 516 R44 v6.1 (Pham et al., 2020).

168 A multiple sequence alignment of 19 *OFP20* haplotypes (Supplemental File 11) was
169 generated using MUSCLE v3.8. Alleles 1–7 and M6_ScOFP20 were reported by van Eck et al.
170 (2022), and the remaining haplotypes come from the dihaploids. The frequency of *OFP20.1* was
171 approximated by ALT frequency at marker OFP20_M6_CDS_994 (994 bp in M6 CDS). For
172 allele *OFP20.8*, which was discovered in the dihaploids (i.e., not in the FASTA file from van
173 Eck et al. (2022)), allele frequency was approximated by REF frequency at marker
174 OFP20_M6_CDS_24; this only works in populations without the M6_ScOFP20 allele. Marker
175 OFP20_M6_CDS_171 was used to report allele depth for allele 2 (ALT) vs. alleles 3 and 7
176 combined (REF); alleles 1 and 8 were not detected by this marker. Marker OFP20_M6_CDS_75
177 was supposed to capture an indel at 82 bp that differentiates alleles 3 and 7, but neither haplotype
178 was present in the MADC file (File S4).

179 **3 RESULTS**

180 **3.1 Genomic markers**

181 Version 1 (V1) of the potato DArTag GBS assay contained 2501 genomic SNPs, which
182 were selected from the 22K V3 potato SNP array to maximize genome coverage and
183 polymorphism rates (i.e., high minor allele frequency). The number of genomic markers per
184 chromosome ranged from 176 on chr12 to 272 on chr01. The mean distance between adjacent
185 markers was 0.35 cM, with the largest gap of 4.77 cM located on chr11 (Figure S2).

186 Analysis of 703 tetraploid samples, from three submissions across three years (2020-2022),
187 revealed variability in the amount of sequencing data per sample. In 2020, the total depth (DP
188 sum over markers) was consistent across samples, with mean 0.53M/sample and standard
189 deviation 0.07M (Figure 1). The distribution in 2021 was bimodal, with the two modes
190 corresponding to different plates. The lower mode was 0.63M, while the higher mode was
191 0.96M. The average total depth in 2022 was similar to 2020, at 0.53M/sample, but the standard
192 deviation was higher, at 0.17M.

193 When sample DP was summarized by marker, the data were more consistent across years
194 (Figure 2). The 10th percentile for mean sample DP was 32, 53, and 24 in years 2020, 2021, and
195 2022, respectively (Fig. 2A). Despite the observed differences in total DP per sample (Figure 1),
196 there was a consistent relationship between the mean (μ) and standard deviation (σ) for sample
197 DP (Fig. 2B). The relationship between these quantities in a Poisson distribution is $\mu = \sigma^{0.5}$,
198 which is a straight line with slope 0.5 on a log-log plot (dashed line in Fig. 2B). The observed
199 data were overdispersed (i.e., more variable) compared to the Poisson, with slope 0.79 (SE 0.00),
200 meaning that $\mu \approx \sigma^{0.8}$.

201 Tetraploid genotype calls were made with R package *updog* (Gerard et al. 2018), which
202 provides estimates of allelic bias (AB) for each marker—a parameter that measures the relative
203 probability of observing the REF vs. ALT allele. When AB=1, or equivalently $\log_2(AB) = 0$,
204 there is no bias. When AB=2, or equivalently $\log_2(AB)=1$, the REF allele is twice as likely to be
205 observed in a balanced heterozygote. 10% of the markers exhibited bias $|(AB)| > 1$ (Figure S3),
206 but many of these still appeared to have reliable clustering (Figure 3).

207 V1 DArTag and SNP array genotypes were compared for 1865 common markers across 298
208 tetraploid clones. Both platforms identified two groups of genetically identical clones, one pair
209 and one threesome, originating from the same F1 populations (Figure S4). This is not uncommon
210 in potato breeding due to how single plant selection is conducted in the first field year. After
211 removing duplicates, the two marker profiles (GBS & array) for every clone were paired under
212 hierarchical clustering (Figure S5), indicating close agreement.

213 For a quantitative comparison, several measures of error were computed for each marker
214 (Supplemental File S12). Classification error (CE), which is the proportion of samples with
215 different genotype calls, was calculated for both tetraploid (4x) and pseudo-diploid (2x)
216 genotypes (where differences in heterozygote allele dosage are ignored). There was a sharp bend
217 in the cumulative distribution for 2x CE at approximately 0.1 error (Figure 4), with 1647 markers
218 below this threshold (88% of those tested). As expected, fewer markers (1302) satisfied 4x CE <
219 0.1 because of the difficulty discriminating between heterozygous genotypes. For 4x genotypes,
220 the root-mean-squared-error (RMSE) of allele dosage is potentially more meaningful than CE,
221 and 1547 markers had RMSE < 0.5 (Figure 4), a somewhat arbitrary threshold selected because
222 it represents the midpoint between integer dosages.

223 Version 2 (V2) of the potato DArTag GBS assay was designed in 2023 and contains 3893
224 genomic SNPs, of which 2144 were included in Version 1. The additional SNPs were selected
225 from the 31K V4 potato SNP array using the same criteria as before. GBS and SNP array
226 genotypes were compared for 2608 common markers across 78 clones (40 tetraploid, 38 diploid).
227 Given the small number of tetraploids, only the 2x CE criterion was computed, and 2341
228 markers had 2x CE < 0.1 (Figure S6; Supplemental File S13).

229

230 **3.2 Imputation**

231 A key role for the DArTag genomic markers is to facilitate imputation to higher density
232 platforms for genomic selection. Among the 298 clones genotyped with both the SNP array and
233 V1 DArTag is a five-parent half-diallel population of 85 clones, with F1 family sizes between 1
234 and 20 (Table 1). Using a leave-one-family-out cross-validation, we compared the accuracy of
235 two imputation methods, Random Forest (RF) vs. Linkage Analysis (LA). Linkage analysis uses
236 a genetic model of recombination and phased parental genotypes to reconstruct progeny in terms
237 of parental haplotypes. The RMSE for imputing 10K SNP array genotypes from DArTag was
238 always lower with LA compared to RF (Table 1), with overall means of 0.15 and 0.95,
239 respectively.

240

241 **3.3 Trait markers**

242 The V1 DArTag assay had two trait markers, targeting two different resistance genes (*Ryadg*,
243 *Rysto*) for the most economically important viral pest of potato: potato virus Y (PVY). Both
244 variants had previously been targeted with KASP markers, and for 93 samples genotyped with

245 both KASP and V1 DArTag, there were 2 discrepancies for presence/absence of *Ry_{adg}* (Table
246 S1).

247 Besides the two PVY markers, the V2 DArTag assay had five additional trait markers with
248 reliable results (Table 1). We had good prior knowledge about the distribution of the PVY and
249 golden cyst nematode (*H1*) resistance genes in our germplasm from other marker systems
250 (SCAR and KASP). Four clones tested positive for the *Ry_{sto}* marker: three were expected based
251 on previous testing, and the fourth was plausible based on its pedigree (Table S2). Many samples
252 tested positive for *Ry_{adg}* and *H1*, which was expected given the high frequency of these variants
253 in the US chip processing germplasm, but the allele dosages for *Ry_{adg}* seemed too high—eight
254 samples were even homozygous tetraploids. To investigate further, we analyzed a partial diallel
255 population (N=123) within the V2 DArTag dataset (Figure S7). Treating the *Ry_{adg}* and *H1*
256 markers as dominant traits, joint linkage analysis identified which parental haplotypes carry the
257 *R* gene (Figure S8), and corrected dosages were determined by reconstructing the progeny in
258 terms of parental haplotypes (Figure 5). Five triplex and two quadriplex calls for *Ry_{adg}* were
259 corrected down to duplex, and the average upward bias was 0.24 dosage. For *H1*, the original
260 calls were more accurate, with an average bias of only 0.05 dosage.

261 Little is known about resistance to potato wart disease (*S. endobioticum*) in US germplasm,
262 but given the prevalence of the disease in other parts of the world (Obidiegwu et al., 2014), it has
263 become a higher priority for molecular breeding. One trait marker targets the *Sen3* resistance
264 gene (Table 1), which was detected in four individuals with a common parent, AW07791-2rus.
265 Based on pedigree information, we believe the resistance was inherited from its maternal parent,
266 PALB0303-1 (Elison et al., 2021).

267 Another trait marker targets *Sli*, a non-S locus F-box protein that disrupts the gametophytic
268 incompatibility system and allows for the development of diploid, inbred lines (Ma et al., 2022;
269 Eggers et al., 2022). The GBS marker showed perfect agreement with prior knowledge for 28
270 diploid samples based on KASP marker screening (Table S3).

271 A trait marker for the maturity gene *CDF1* targets the location of the 7 bp indel variants that
272 differentiate alleles 2 and 4 from wild-type alleles, collectively designated group 1. Because of
273 the multi-allelic nature of this variant, correct interpretation requires use of the DArT “missing
274 allele discovery count” (MADC) file, which contains read counts for 81 bp haplotypes
275 surrounding each target variant. Five CDF1 haplotypes were detected in the population (Figure
276 6A): three were full-length variants of CDF1.1 (Ref, Other1, Other2), one was CDF1.4 (Alt), and
277 one was CDF1.2 (Other3). The validity of the assay was confirmed by comparing the read counts
278 with samples of known CDF1 genotype (Figure 6B), with the complication that CDF1.3, which
279 has an 865 bp transposon insertion at the same position, is not detected. As a result, samples with
280 zero (or near zero, due to sequencing error) counts are interpreted as homozygous for allele 3.
281 And since clones selected under long-day conditions are typically not homozygous wild-type,
282 when CDF1.1 alleles are detected but not alleles 2 or 4, the predicted genotype is 1/3.

283 Several markers were included in the V2 panel to target *OFP20*, an ovate family protein
284 with a major effect on tuber shape (Wu et al. 2018). This is a complex locus with dozens of
285 predicted alleles (van Eck et al. 2022), so the following approach to interpreting the DArTTag
286 markers may not work in all germplasm groups. Marker OFP20_M6_CDS_994 was used to
287 estimate the frequency of *OFP20.1*, which is the most common allele in cultivated germplasm
288 and promotes elongated shape (van Eck et al. 2022). *OFP20.1* was present at a higher frequency
289 in the russet (N=21) vs. chip (N=300) samples from the UW breeding program (Fig. 7A), which

290 is consistent with the long vs. round tuber phenotypes required for those market types. Marker
291 OFP20_M6_CDS_24 was used to estimate the frequency of *OFP20.8*, which was present in 13%
292 of the chip samples. Together with OFP20_M6_CDS_171, which provided information about
293 presence/absence of *OFP20* alleles 2, 3, and 7, the DArTag markers were able to correctly
294 predict five different *OFP20* genotypes (Fig. 7B).

295 **4 DISCUSSION**

296 The potato DArTag assay has several applications in potato breeding. For its price point, an
297 ideal stage of deployment is the first clonal evaluation trial (CET), which typically occurs in the
298 second field year of potato breeding and may have several thousand clones. The DArTag
299 genomic markers provide a genetic fingerprint that can be used to correct pedigree errors (Muñoz
300 et al., 2014; Endelman et al., 2017) and provide a reference genotype for quality control. The
301 clonal trial entries are also candidates for genomic selection, both as potential clonal varieties
302 and as parents to begin the next breeding cycle (Slater et al., 2016; Wu et al., 2023). Limited
303 phenotyping for some traits occurs in the CET, and a genomic relationship matrix computed
304 from DArTag markers could enable a multi-location trial to better estimate genetic values for the
305 target population of environments, i.e., “sparse testing” (Endelman et al. 2014; Jarquin et al.
306 2020).

307 Based on previous studies, we expect higher selection accuracy if DArTag markers are first
308 imputed to higher density (Cleveland and Hickey, 2013; Gorjanc et al., 2017). The exploitation
309 of pedigree or family structure during marker imputation in diploids is well documented, with a
310 range of methods and software available depending on the structure of the dataset (Meuwissen
311 and Goddard, 2010; Swarts et al., 2014; Hickey et al., 2015; Whalen et al., 2018; Whalen et al.,
312 2020). The present study has confirmed our hypothesis that linkage analysis is also beneficial for
313 imputation in autopolyploids. DArTag panels are available for several autopolyploid crops
314 besides potato, including alfalfa, blueberry, and sweetpotato (Breeding Insight, 2023), so the
315 software developed for this study (Endelman, 2023b) should benefit other breeding communities.
316 Based on the current functionality of the PolyOrigin software (Zheng et al., 2021), only bi-allelic
317 SNPs were used for imputation, but the DArTag missing allele discovery count (MADC) file

318 offers the possibility of using multi-allelic markers, which are generally more informative for
319 linkage analysis (Luo et al., 2001).

320 DArTag is not the only option for mid-density genotyping. The PlexSeq platform (AgriPlex,
321 Cleveland, USA) is also widely used, for example in soybean and pearl millet (Semalaiyappan et
322 al., 2023). Leyva Pérez et al. (2022) developed their own targeted GBS platform for potato,
323 PotatoMASH, but the number of genomic markers (339) was small compared to the options with
324 DArTag and PlexSeq.

325 Besides more genomic markers, a major advantage of the V2 DArTag assay is the additional
326 trait markers (Table 2). It is very valuable to select for resistance to three important pests of
327 potato—PVY, wart, and golden cyst nematode—with the same assay used for genomic selection.
328 Notably absent from this list is potato late blight, caused by the pathogen *P. infestans*. Trait
329 marker *blb1*_chr08_51070621 was designed to target the *RB/Rpi-blb1* gene (Song et al., 2003;
330 van der Vossen et al., 2003) based on a SNP in the 3'UTR that worked well as a KASP marker
331 (Sorensen et al., 2023). However, no haplotypes were detected in the V2 DArTag experiment for
332 three positive samples from the KASP study. The V2 assay also targeted two genes affecting
333 tuber skin color: *f3* '5'h (Jung et al., 2005) and *an2* (Jung et al., 2009). Both loci have complex
334 allelic series (Hoopes et al. 2022), and more information is needed about their functional effects
335 to guide selection. For tuber shape, we confirmed one trait marker estimates the frequency of the
336 most common long allele, *OFP20.1*. This marker can have an immediate impact on parent
337 selection in the russet market type, where round alleles are undesirable due to their partial
338 dominance.

339 **FIGURE CAPTIONS**

340 **Figure 1.** Total depth per sample, in million (M) read counts, for three submissions of potato V1
341 DArTag.

342

343 **Figure 2.** (A) Distribution of the mean sample depth (DP) for V1 DArTag markers. (B) Log-log
344 plot of the relationship between the standard deviation and mean for sample DP. Individual
345 marker points are shown only for 2021 to maintain legibility. Combining the data across years,
346 the overall regression line (not shown) has slope 0.79 (SE 0.00) and $R^2 = 0.99$.

347

348 **Figure 3.** Examples of DArTag markers without (A) vs. with (B) allelic bias. Dashed lines
349 correspond to possible tetraploid allele ratios when there is no allelic bias (1:0, 3:1, 1:1, 1:3, 0:1).
350 (A) solcap.snp_c2_36615 with bias = -0.2. (B) PotVar0072076 with bias = 1.8.

351

352 **Figure 4.** Empirical cumulative distribution for the error between the V1 DArTag and SNP array
353 on 1865 common markers. CE = classification error. RMSE = root-mean-squared-error. 2x =
354 pseudo-diploid genotypes. 4x = tetraploid genotypes.

355

356 **Figure 5.** Original vs. corrected genotypes for the trait markers Ryadg_chr11_2499502 and
357 H1_chr05_52349069. The original genotypes were based on R/updog with a “norm” prior and
358 then corrected based on linkage analysis.

359

360 **Figure 6.** (A) Multiple sequence alignment of the DArTag haplotypes discovered for trait marker
361 CDF1.4_chr05_448021. Haplotypes Ref, Other1, Other2 are CDF1.1 alleles, while Alt is
362 CDF1.4 and Other3 is CDF1.2. (B) Haplotype read counts for samples with known CDF1
363 genotype.

364

365 **Figure 7.** (A) Distribution of sample allele frequencies for OFP20.1 in round chip (N=300) vs.
366 long russet (N=21) germplasm. (B) Comparison of known OFP20 genotypes with V2 DArT
367 markers. Allele frequency (AF) of OFP20.1 was approximated by ALT frequency at marker
368 OFP20_M6_CDS_994. AF of OFP20.8 was approximated by REF frequency at marker

369 OFP20_M6_CDS_24. Allele depth (AD) at OFP20_M6_CDS_171 was used to distinguish allele
370 2 (ALT) from alleles 3 and 7 (REF).

371

372

373

374 **TABLES**

375 **Table 1.** Half-diallel population with five parents. Above diagonal: F1 population sizes; Below
376 diagonal: imputation root-mean-squared-error with linkage analysis (blue, top) vs. random forest
377 (red, bottom).

	P1	P2	P3	P4	P5
P1		3	5	9	20
P2	0.14 0.95		8	1	9
P3	0.15 0.95	0.17 0.96		7	11
P4	0.13 0.95	0.14 0.93	0.13 0.94		12
P5	0.16 0.95	0.16 0.96	0.14 0.94	0.15 0.95	

378

379 **Table 2.** Validated trait markers in the V2 DArTag assay.

Marker	Target Gene (Trait)	Functional	Reference
		Allele	
Rysto_chr12_2352742	<i>Ry_{sto}</i> (PVY)	REF ^a	Nie et al. (2016)
Ryadg_chr11_2499502	<i>Ry_{adg}</i> (PVY)	ALT	Herrera et al. (2018)
H1_chr05_52349069	<i>H1</i> (golden cyst nematode)	ALT	Meade et al. (2020)
Sen3_chr11_2563398	<i>Sen3</i> (wart)	ALT	Prodhomme et al. (2019)
Sli_chr12_2372490	<i>Sli</i> (self-compatibility)	ALT	Clot et al. (2020)
CDF1.4_chr05_4488021	<i>CDF1</i> (maturity)	N/A	Gutaker et al. (2019)
OFP20_M6_CDS_24 OFP20_M6_CDS_171 OFP20_M6_CDS_994	<i>OFP20</i> (tuber shape)	N/A	van Eck et al. (2022)

380 ^aThe REF/ALT designation for Rysto_chr12_2352742 is reversed compared to the original design file
381 based on the DMv6.1 reference genome. As a result, the functional allele is REF.

382

383 **SUPPLEMENTAL FILES**

384 During peer review, the supplemental files are available from the Dryad Digital Repository at

385 https://datadryad.org/stash/share/tdvUt18gBCz6bJ568DaE7mLrWtq55kZzJa_C1uLYSfQ. The

386 permanent link for the supplemental files after publication is

387 <https://doi.org/10.5061/dryad.8pk0p2nw4>.

388

389 File S1. Potato DArTag V1 data for 703 samples (VCF).

390 File S2. Metadata with year submission for the samples in File S1 (CSV).

391 File S3. Potato DArTag V2 data for 375 samples (VCF).

392 File S4. DArT Missing Allele Discovery Counts for the samples in File S3 (CSV).

393 File S5. Potato V4 SNP array data for 298 samples (VCF).

394 File S6. Pedigree for diallel population in the V1 DArTag dataset (CSV).

395 File S7. Phased parental genotypes for the diallel population in File S6 (CSV).

396 File S8. Pedigree for diallel population in the V2 DArTag dataset (CSV).

397 File S9. Parental genotype probabilities for the diallel population in File S8 (CSV).

398 File S10. Trait marker phenotypes for the diallel population in File S8 (CSV).

399 File S11. Sequence alignment and percent identity matrix for *OFP20* (DOCX).

400 File S12. Marker concordance between V1 DArTag and the SNP array (CSV).

401 File S13. Marker concordance between V2 DArTag and the SNP array (CSV).

402 **AUTHOR CONTRIBUTIONS**

403 **Jeffrey B. Endelman:** Conceptualization, Resources, Investigation, Formal analysis, Software,
404 Supervision, Writing – original draft. **Moctar Kante:** Conceptualization, Resources,
405 Investigation, Formal analysis, Writing – original draft. **Hannele Lindqvist-Kreuze:**
406 Conceptualization, Resources, Supervision. **Andrzej Kilian:** Methodology. **Laura M. Shannon:**
407 Conceptualization, Supervision. **Maria V. Caraza-Harter:** Resources. **Brieanne Vaillancourt:**
408 Formal analysis, Data curation. **Kathrine Mailloux:** Investigation, Resources. **John P.**
409 **Hamilton:** Formal analysis. **C. Robin Buell:** Conceptualization, Supervision. **All authors:**
410 Writing – review & editing.

411

412 **ACKNOWLEDGMENTS**

413 Development of the V1 DArTag panel was supported by the CGIAR Excellence in Breeding
414 Platform and Crops to End Hunger Initiative. The USDA National Institute of Food &
415 Agriculture (NIFA) Award 2019-51181-30021 supported development of the V2 DArTag panel,
416 with additional support from PepsiCo for the development of genomic resources to validate
417 markers. Genotyping of UW-Madison potato breeding lines was supported by USDA NIFA
418 Awards 2020-51181-32156 and 2021-34141-35447. We thank D. DeKooyer for suggesting the
419 marker for *Sen3* resistance.

420

421 **CONFLICT OF INTEREST STATEMENT**

422 J. Endelman is a member of the editorial board for *The Plant Genome*. A. Kilian is an employee
423 of Diversity Arrays Technology, the company that provides the DArTag genotyping service.

424

425 **DATA AVAILABILITY STATEMENT**

426 Supplemental Files S1 – S10, which contain the marker and pedigree data needed to reproduce
427 the results of this study, will be available from the Dryad Digital Repository at
428 <https://doi.org/10.5061/dryad.8pk0p2nw4> upon publication. Upon manuscript acceptance,
429 PacBio HiFi sequencing data will be available via the NCBI Sequence Read Archive under
430 BioSamples SAMN38982152, SAMN38982165, SAMN38982166, SAMN38982167, and
431 SAMN38982169, and Illumina sequencing data will be available via the NCBI Sequence Read
432 Archive under BioSamples SAMN39419651, SAMN39670896, SAMN39670897, and
433 SAMN39670898.

434 **REFERENCES**

435 Ali, O.A., O'Rourke, S.M., Amish, S.J., Meek, M.H., Luikart, G., Jeffres, C., & Miller, M.R.
436 (2016). Rad capture (Rapture): Flexible and efficient sequence-based genotyping. *Genetics*,
437 202, 389–400. <https://doi.org/10.1534/genetics.115.183665>

438 Alonge, M., Soyk, S., Ramakrishnan, S. (2019). RaGOO: fast and accurate reference-guided
439 scaffolding of draft genomes. *Genome Biology*, 20, 224. <https://doi.org/10.1186/s13059-019-1829-6>

440 Amadeu, R.R., Muñoz, P.R., Zheng, C., & Endelman, J.B. (2021). QTL mapping in outbred
441 tetraploid (and diploid) diallel populations. *Genetics*, 219, iyab124.
442 <https://doi.org/10.1093/genetics/iyab124>

443 Baird, N.A., Etter, P.D., Atwood, T.S., Currey, M.C., Shiver, A.L., Lewis, Z.A., Selker, E.U.,
444 Cresko, W.A., & Johnson, E.A. (2008). Rapid SNP discovery and genetic mapping using
445 sequenced RAD markers. *PLoS ONE*, 3, e3376.
446 <https://doi.org/10.1371/journal.pone.0003376>

447 Bastien, M., Boudhrioua, C., Fortin, G., Belzile, F., & Phillips, D.W. (2018). Exploring the
448 potential and limitations of genotyping-by-sequencing for SNP discovery and genotyping in
449 tetraploid potato. *Genome*, 61, 449–456. <https://doi.org/10.1139/gen-2017-0236>

450 Breeding Insight (2023). Open Source Genetic Marker Panels.
451 <https://breedinginsight.org/breeding-solutions/open-source-dartag-marker-panels/> (Accessed
452 29 December 2023).

453 de Bem Oliveira, I., Resende, M.F.R., Ferrão, L.F. V., Amadeu, R.R., Endelman, J.B., Kirst, M.,
454 Coelho, A.S.G., & Munoz, P.R. (2019). Genomic prediction of autotetraploids; influence of
455 relationship matrices, allele dosage, and continuous genotyping calls in phenotype
456 prediction. *G3: Genes, Genomes, Genetics*, 9, 1189–1198.
457 <https://doi.org/10.1534/g3.119.400059>

458 Campbell, N.R., Harmon, S.A., & Narum, S.R. (2015). Genotyping-in-Thousands by sequencing
459 (GT-seq): A cost effective SNP genotyping method based on custom amplicon sequencing.
460 *Molecular Ecology Resources*, 15, 855–867. <https://doi.org/10.1111/1755-0998.12357>

461 Cheng, H., Concepcion, G.T., Feng, X., Zhang, H., & Li H. (2021). Haplotype-resolved de
462 novo assembly using phased assembly graphs with hifiasm. *Nature Methods*, 18, 170-175.
463 <https://doi.org/10.1038/s41592-020-01056-5>

464 Cheng, H., Jarvis, E.D., Fedrigo, O., Koepfli, K.P., Urban, L., Gemmell, N.J., & Li, H. (2022).
465 Haplotype-resolved assembly of diploid genomes without parental data. *Nature
466 Biotechnology*, 40, 1332–1335. <https://doi.org/10.1038/s41587-022-01261-x>

467 Cleveland, M.A., & Hickey, J.M. (2013). Practical implementation of cost-effective genomic
468 selection in commercial pig breeding using imputation. *Journal of Animal Science*, 91,
469 3583–3592. <https://doi.org/10.2527/jas2013-6270>

470 Danecek, P., Bonfield, J.K., Liddle, J., Marshall, J., Ohan, V., Pollard, M.O., Whitwham, A.,
471 Keane, T., McCarthy, S.A., & Davies, R.M. (2021). Twelve years of SAMtools and
472 BCFtools. *GigaScience*, 10. <https://doi.org/10.1093/gigascience/giab008>

473 Edgar, R.C. (2004). MUSCLE: multiple sequence alignment with high accuracy and high
474 throughput. *Nucleic Acids Research*, 32, 1792–1797. <https://doi.org/10.1093/nar/gkh340>

475 Eggers, E.J., van der Burgt, A., van Heusden, S.A.W., de Vries, M.E., Visser, R.G.F., Bachem,
476 C.W.B., & Lindhout, P. (2021). Neofunctionalisation of the Sli gene leads to self-
477

478 compatibility and facilitates precision breeding in potato. *Nature Communications*, 12.
479 <https://doi.org/10.1038/s41467-021-24267-6>

480 Elison, G.L., Novy, R.G., & Whitworth, J.L. (2021). Russet Potato Breeding Clones with
481 Extreme Resistance to Potato Virus Y Conferred by Rychc as well as Resistance to Late
482 Blight and Cold-Induced Sweetening. *American Journal of Potato Research*, 98, 411–419.
483 <https://doi.org/10.1007/s12230-021-09852-1>

484 Elshire, R.J., Glaubitz, J.C., Sun, Q., Poland, J. a, Kawamoto, K., Buckler, E.S., & Mitchell, S.E.
485 (2011). A robust, simple genotyping-by-sequencing (GBS) approach for high diversity
486 species. *PloS ONE*, 6, e19379. <https://doi.org/10.1371/journal.pone.0019379>

487 Endelman, J.B. (2023a). R/MapRtools. <https://github.com/jendelman/MapRtools> (version 0.32)

488 Endelman, J.B. (2023b). R/polyBreedR. <https://github.com/jendelman/polyBreedR> (version
489 0.36)

490 Endelman, J.B., Atlin, G.N., Beyene, Y., Semagn, K., Zhang, X., Sorrells, M.E., & Jannink, J.L.
491 (2014). Optimal design of preliminary yield trials with genome-wide markers. *Crop Science*,
492 54, 48–59. <https://doi.org/10.2135/cropsci2013.03.0154>

493 Endelman, J.B., & Jansky, S.H. (2016). Genetic mapping with an inbred line-derived F2
494 population in potato. *Theoretical and Applied Genetics*, 129, 935–943.
495 <https://doi.org/10.1007/s00122-016-2673-7>

496 Endelman, J.B., Schmitz Carley, C.A., Bethke, P.C., Coombs, J.J., Clough, M.E., da Silva, W.L.,
497 De Jong, W.S., Douches, D.S., Frederick, C.M., Haynes, K.G., Holm, D.G., Miller, J.C.,
498 Muñoz, P.R., Navarro, F.M., Novy, R.G., Palta, J.P., Porter, G.A., Rak, K.T., Sathuvalli,
499 V.R., Thompson, A.L., & Yencho, G.C. (2018). Genetic variance partitioning and Genome-
500 wide prediction with allele dosage information in autotetraploid potato. *Genetics*, 209, 77–
501 87. <https://doi.org/10.1534/genetics.118.300685>

502 Endelman, J.B., Schmitz Carley, C.A., Douches, D.S., Coombs, J.J., Bizimungu, B., De Jong,
503 W.S., Haynes, K.G., Holm, D.G., Miller, J.C., Novy, R.G., Palta, J.P., Parish, D.L., Porter,
504 G.A., Sathuvalli, V.R., Thompson, A.L., & Yencho, G.C. (2017). Pedigree Reconstruction
505 with Genome-Wide Markers in Potato. *American Journal of Potato Research*, 94, 184–190.
506 <https://doi.org/10.1007/s12230-016-9556-y>

507 Excellence in Breeding (2022). Mid-density genotyping service.
508 <https://excellenceinbreeding.org/toolbox/services/mid-density-genotyping-service>
509 (accessed 29 December 2023)

510 Felcher, K.J., Coombs, J.J., Massa, A.N., Hansey, C.N., Hamilton, J.P., Veilleux, R.E., Buell,
511 C.R., & Douches, D.S. (2012). Integration of two diploid potato linkage maps with the
512 potato genome sequence. *PloS ONE*, 7, e36347.
513 <https://doi.org/10.1371/journal.pone.0036347>

514 Fu, A., Narasimhan, B., & Boyd, S. (2020). CVXR: An R package for disciplined convex
515 optimization. *Journal of Statistical Software*, 94, 1–34. <https://doi.org/10.18637/jss.v094.i14>

516 Gasc, C., Peyretailade, E., & Peyret, P. (2016). Sequence capture by hybridization to explore
517 modern and ancient genomic diversity in model and nonmodel organisms. *Nucleic Acids
518 Research*, 44, 4504–4518. <https://doi.org/10.1093/nar/gkw309>

519 Gerard, D., Ferrão, L.F.V., Garcia, A.A.F., & Stephens, M. (2018). Genotyping polyploids from
520 messy sequencing data. *Genetics*, 210, 789–807.
521 <https://doi.org/10.1534/genetics.118.301468>

522 Gorjanc, G., Battagin, M., Dumasy, J.F., Antolin, R., Gaynor, R.C., & Hickey, J.M. (2017).
523 Prospects for cost-effective genomic selection via accurate within-family imputation. *Crop*
524 *Science*, 57, 216–228. <https://doi.org/10.2135/cropsci2016.06.0526>

525 Gutaker, R.M., Weiß, C.L., Ellis, D., Anglin, N.L., Knapp, S., Luis Fernández-Alonso, J., Prat,
526 S., & Burbano, H.A. (2019). The origins and adaptation of European potatoes reconstructed
527 from historical genomes. *Nature Ecology and Evolution*, 3, 1093–1101.
528 <https://doi.org/10.1038/s41559-019-0921-3>

529 Hamilton, J.P., Hansey, C.N., Whitty, B.R., Stoffel, K., Massa, A.N., Deynze, A. Van, Jong,
530 W.S. De, Douches, D.S., & Buell, C.R. (2011). Single nucleotide polymorphism discovery
531 in elite North American potato germplasm. *BMC Genomics*, 302. <https://doi.org/10.1186/1471-2164-12-302>

532 Hardenbol, P., Banér, J., Jain, M., Nilsson, M., Namsaraev, E.A., Karlin-Neumann, G.A.,
533 Fakhrai-Rad, H., Ronaghi, M., Willis, T.D., Landegren, U., & Davis, R.W. (2003)
534 Multiplexed genotyping with sequence-tagged molecular inversion probes. *Nature*
535 *Biotechnology*, 21, 673–678. <https://doi.org/10.1038/nbt821>

536 Hardigan, M.A., Feldmann, M.J., Carling, J., Zhu, A., Kilian, A., Famula, R.A., Cole, G.S., &
537 Knapp, S.J. (2023). A medium-density genotyping platform for cultivated strawberry using
538 DArTag technology. *Plant Genome*, 16. <https://doi.org/10.1002/tpg2.20399>

539 Herrera, M. del R., Vidalon, L.J., Montenegro, J.D., Riccio, C., Guzman, F., Bartolini, I., &
540 Ghislain, M. (2018). Molecular and genetic characterization of the Ryadg locus on
541 chromosome XI from Andigena potatoes conferring extreme resistance to potato virus Y.
542 *Theoretical and Applied Genetics*, 131, 1925–1938. <https://doi.org/10.1007/s00122-018-3123-5>

543 Hickey, J.M., Gorjanc, G., Varshney, R.K., & Nettelblad, C. (2015). Imputation of single
544 nucleotide polymorphism genotypes in biparental, backcross, and topcross populations with
545 a hidden markov model. *Crop Science*, 55, 1934–1946.
546 <https://doi.org/10.2135/cropsci2014.09.0648>

547 Jarquin, D., Howard, R., Crossa, J., Beyene, Y., Gowda, M., Martini, J.W.R., Pazaran, G.C.,
548 Burgueño, J., Pacheco, A., Grondona, M., Wimmer, V., & Prasanna, B.M. (2020). Genomic
549 prediction enhanced sparse testing for multi-environment trials. *G3: Genes, Genomes,*
550 *Genetics*, 10, 2725–2739. <https://doi.org/10.1534/g3.120.401349>

551 Jung, C.S., Griffiths, H.M., De Jong, D.M., Cheng, S., Bodis, M., & De Jong, W.S. (2005). The
552 potato P locus codes for flavonoid 3',5'-hydroxylase. *TAG. Theoretical and Applied*
553 *Genetics*, 110, 269–75. <https://doi.org/10.1007/s00122-004-1829-z>

554 Jung, C.S., Griffiths, H.M., De Jong, D.M., Cheng, S., Bodis, M., Kim, T.S., & De Jong, W.S.
555 (2009). The potato developer (D) locus encodes an R2R3 MYB transcription factor that
556 regulates expression of multiple anthocyanin structural genes in tuber skin. *Theoretical and*
557 *Applied Genetics*, 120, 45–57. <https://doi.org/10.1007/s00122-009-1158-3>

558 Kloosterman, B., Abelenda, J. a, Gomez, M.D.M.C., Oortwijn, M., de Boer, J.M., Kowitwanich,
559 K., Horvath, B.M., van Eck, H.J., Smacznak, C., Prat, S., Visser, R.G.F., & Bachem,
560 C.W.B. (2013). Naturally occurring allele diversity allows potato cultivation in northern
561 latitudes.. *Nature*, 495, 246–50. <https://doi.org/10.1038/nature11912>

562 Knaus, B.J., & Grünwald, N.J. (2017). VCFR: a package to manipulate and visualize variant call
563 format data in R. *Molecular Ecology Resources*, 17, 44–53. <https://doi.org/10.1111/1755-0998.12549>

567 Leyva-Pérez, M. de la O., Vexler, L., Byrne, S., Clot, C.R., Meade, F., Griffin, D., Ruttink, T.,
568 Kang, J., & Milbourne, D. (2022). PotatoMASH—A Low Cost, Genome-Scanning Marker
569 System for Use in Potato Genomics and Genetics Applications. *Agronomy*, 12.
570 <https://doi.org/10.3390/agronomy12102461>

571 Liaw, A., & Wiener, M. (2002). Classification and regression by randomForest. *R News*, 2, 18–
572 22. <https://doi.org/10.1177/154405910408300516>

573 Luo, Z.W., Hackett, C.A., Bradshaw, J.E., McNicol, J.W., & Milbourne, D. Construction of a
574 Genetic Linkage Map in Tetraploid Species Using Molecular Markers. *Genetics*, 157, 1369–
575 1385.

576 Ma, L., Zhang, C., Zhang, B., Tang, F., Li, F., Liao, Q., Tang, D., Peng, Z., Jia, Y., Gao, M.,
577 Guo, H., Zhang, J., Luo, X., Yang, H., Gao, D., Lucas, W.J., Li, C., Huang, S., & Shang, Y.
578 (2021). A nonS-locus F-box gene breaks self-incompatibility in diploid potatoes. *Nature
579 Communications*, 12. <https://doi.org/10.1038/s41467-021-24266-7>

580 Matias, F.I., Xavier Meireles, K.G., Nagamatsu, S.T., Lima Barrios, S.C., Borges do Valle, C.,
581 Carazzolle, M.F., Fritsche-Neto, R., & Endelman, J.B. (2019). Expected Genotype Quality
582 and Diploidized Marker Data from Genotyping-by-Sequencing of *Urochloa spp.*
583 Tetraploids. *The Plant Genome*, 12. <https://doi.org/10.3835/plantgenome2019.01.0002>

584 Meuwissen, T., & Goddard, M. (2010). The use of family relationships and linkage
585 disequilibrium to impute phase and missing genotypes in up to whole-genome sequence
586 density genotypic data. *Genetics*, 185, 1441–1449.
587 <https://doi.org/10.1534/genetics.110.113936>

588 Muñoz, P.R., Resende, M.F.R., Huber, D.A., Quesada, T., Resende, M.D.V., Neale, D.B.,
589 Wegrzyn, J.L., Kirst, M., & Peter, G.F. (2014). Genomic relationship matrix for correcting
590 pedigree errors in breeding populations: Impact on genetic parameters and genomic
591 selection accuracy. *Crop Science*, 54, 1115–1123.
592 <https://doi.org/10.2135/cropsci2012.12.0673>

593 Nie, X., Sutherland, D., Dickison, V., Singh, M., Murphy, A.M., & De Koeyer, D. (2016).
594 Development and validation of high-resolution melting markers derived from Rysto STS
595 markers for high-throughput marker-assisted selection of potato carrying Rysto.
596 *Phytopathology*, 106, 1366–1375. <https://doi.org/10.1094/PHYTO-05-16-0204-R>

597 Obidiegwu, J.E., Flath, K., & Gebhardt, C. (2014). Managing potato wart: A review of present
598 research status and future perspective. *Theoretical and Applied Genetics*, 127, 763–780.
599 <https://doi.org/10.1007/s00122-014-2268-0>

600 Pham, G.M., Hamilton, J.P., Wood, J.C., Burke, J.T., Zhao, H., Vaillancourt, B., Ou, S., Jiang,
601 J., & Robin Buell, C. (2020). Construction of a chromosome-scale long-read reference
602 genome assembly for potato. *GigaScience*, 9. <https://doi.org/10.1093/gigascience/giaa100>

603 Prodhomme, C., Esselink, D., Borm, T., Visser, R.G.F., Van Eck, H.J., & Vossen, J.H. (2019).
604 Comparative Subsequence Sets Analysis (CoSSA) is a robust approach to identify haplotype
605 specific SNPs; Mapping and pedigree analysis of a potato wart disease resistance gene *Sen3*.
606 *Plant Methods*, 15. <https://doi.org/10.1186/s13007-019-0445-5>

607 Semalaiyappan, J., Selvanayagam, S., Rathore, A., Gupta, S.K., Chakraborty, A., Gujjula, K.R.,
608 Haktan, S., Viswanath, A., Malipatil, R., Shah, P., Govindaraj, M., Ignacio, J.C., Reddy, S.,
609 Singh, A.K., & Thirunavukkarasu, N. (2023). Development of a new AgriSeq 4K mid-
610 density SNP genotyping panel and its utility in pearl millet breeding. *Frontiers in Plant
611 Science*, 13. <https://doi.org/10.3389/fpls.2022.1068883>

612 Shen, W., Le, S., Li, Y., & Hu, F. (2016). SeqKit: a cross-platform and ultrafast toolkit for
613 FASTA/Q file manipulation. *PLoS ONE*, 11, e0163962.
614 <https://doi.org/10.1371/journal.pone.0163962>

615 Sharma, S.K., & Bryan, G.J. (2017). Genome Sequence-Based Marker Development and
616 Genotyping in Potato. In S. Kumar Chakrabarti, C. Xie & J. Kumar Tiwari (Eds.), *The*
617 *Potato Genome. Compendium of Plant Genomes* (pp. 307–326). Springer.

618 Slater, A.T., Cogan, N.O.I., Forster, J.W., Hayes, B.J., & Daetwyler, H.D. (2016). Improving
619 Genetic Gain with Genomic Selection in Autotetraploid Potato. *The Plant Genome*, 9.
620 <https://doi.org/10.3835/plantgenome2016.02.0021>

621 Song, J., Bradeen, J.M., Kristine Naess, S., Raasch, J.A., Wielgus, S.M., Haberlach, G.T., Liu, J.,
622 Kuang, H., Austin-Phillips, S., Robin Buell, C., Helgeson, J.P., & Jiang, J. (2003). Gene *RB*
623 cloned from *Solanum bulbocastanum* confers broad spectrum resistance to potato late blight.
624 *Proceedings of the National Academy of Sciences*, 100, 9128–9133.

625 Song, L., & Endelman, J.B. (2023). Using haplotype and QTL analysis to fix favorable alleles in
626 diploid potato breeding. *The Plant Genome*, e20339. <https://doi.org/10.1002/tpg2.20339>

627 Sorensen, P.L., Christensen, G., Karki, H.S., & Endelman, J.B. (2023). A KASP Marker for the
628 Potato Late Blight Resistance Gene *RB/Rpi-blb1*. *American Journal of Potato Research*,
629 100, 240–246. <https://doi.org/10.1007/s12230-023-09914-6>

630 Swarts, K., Li, H., Romero Navarro, J.A., An, D., Romay, M.C., Hearne, S., Acharya, C.,
631 Glaubitz, J.C., Mitchell, S., Elshire, R.J., Buckler, E.S., & Bradbury, P.J. (2014). Novel
632 Methods to Optimize Genotypic Imputation for Low-Coverage, Next-Generation Sequence
633 Data in Crop Plants. *The Plant Genome*, 7.
634 <https://doi.org/10.3835/plantgenome2014.05.0023>

635 Uitdewilligen, J.G.A.M.L., Wolters, A.A., Bjorn, B.D., Borm, T.J.A., Visser, R.G.F., & Eck,
636 H.J. Van. (2013). A Next-Generation Sequencing Method for Genotyping- by-Sequencing
637 of Highly Heterozygous Autotetraploid Potato, *PLoS ONE*, 8, e0141940.
638 <https://doi.org/10.1371/journal.pone.0062355>

639 Vaillancourt, B., & Buell, C.R. (2019). High molecular weight DNA isolation method from
640 diverse plant species for use with Oxford Nanopore sequencing. *bioRxiv*, 783159.
641 <https://doi.org/10.1101/783159>.

642 Voorrips, R.E., Gort, G., & Vosman, B. (2011). Genotype calling in tetraploid species from bi-
643 allelic marker data using mixture models.. *BMC Bioinformatics*, 12, 172.
644 <https://doi.org/10.1186/1471-2105-12-172>

645 Vos, P.G., Uitdewilligen, J.G.A.M.L., Voorrips, R.E., Visser, R.G.F., & van Eck, H.J. (2015).
646 Development and analysis of a 20K SNP array for potato (*Solanum tuberosum*): an insight
647 into the breeding history. *Theoretical and Applied Genetics*, 128, 2387–2401.
648 <https://doi.org/10.1007/s00122-015-2593-y>

649 van der Vossen, E., Sikkema, A., Te Lintel Hekkert, B., Gros, J., Stevens, P., Muskens, M.,
650 Wouters, D., Pereira, A., Stiekema, W., & Allefs, S. (2003). An ancient R gene from the
651 wild potato species *Solanum bulbocastanum* confers broad-spectrum resistance to
652 *Phytophthora infestans* in cultivated potato and tomato. *Plant Journal*, 36, 867–882.
653 <https://doi.org/10.1046/j.1365-313X.2003.01934.x>

654 van Eck, H.J., Oortwijn, M.E.P., Terpstra, I.R., van Lieshout, N.H.M., van der Knaap, E.,
655 Willemse, J.H., & Bachem, C.W.B. (2022). Engineering of tuber shape in potato (*Solanum*
656 *tuberosum*) with marker assisted breeding or genetic modification using StOFP20. *Research*
657 *Square, PREPRINT*. <https://doi.org/10.21203/rs.3.rs-1807189/v1>

658 Wang, W., & Yan, J. (2021). Shape-Restricted Regression Splines with R Package splines2.
659 *Journal of Data Science*, 498–517. <https://doi.org/10.6339/21-JDS1020>

660 Whalen, A., Gorjanc, G., & Hickey, J.M. (2020). AlphaFamImpute: High-accuracy imputation in
661 full-sib families from genotype-by-sequencing data. *Bioinformatics*, 36, 4369–4371.
662 <https://doi.org/10.1093/bioinformatics/btaa499>

663 Whalen, A., Ros-Freixedes, R., Wilson, D.L., Gorjanc, G., & Hickey, J.M. (2018). Hybrid
664 peeling for fast and accurate calling, phasing, and imputation with sequence data of any
665 coverage in pedigrees. *Genetics Selection Evolution*, 50. <https://doi.org/10.1186/s12711-018-0438-2>

666

667 Wu, P.Y., Stich, B., Renner, J., Muders, K., Prigge, V., & van Inghelandt, D. (2023). Optimal
668 implementation of genomic selection in clone breeding programs—Exemplified in potato: I.
669 Effect of selection strategy, implementation stage, and selection intensity on short-term
670 genetic gain. *Plant Genome*, 16. <https://doi.org/10.1002/tpg2.20327>

671 Wu, S., Zhang, B., Keyhaninejad, N., Rodríguez, G.R., Kim, H.J., Chakrabarti, M., Illa-
672 Berenguer, E., Taitano, N.K., Gonzalo, M.J., Díaz, A., Pan, Y., Leisner, C.P., Halterman, D.,
673 Buell, C.R., Weng, Y., Jansky, S.H., van Eck, H., Willemsen, J., Monforte, A.J., Meulia, T.,
674 & van der Knaap, E. (2018). A common genetic mechanism underlies morphological
675 diversity in fruits and other plant organs. *Nature Communications*, 9.
676 <https://doi.org/10.1038/s41467-018-07216-8>

677 Zhao, D., Mejia-Guerra, K.M., Mollinari, M., Samac, D., Irish, B., Heller-Uszynska, K., Beil,
678 C.T., & Sheehan, M.J. (2023). A public mid-density genotyping platform for alfalfa
679 (*Medicago sativa* L.). *Genetic Resources*, 4, 55–63.
680 <https://doi.org/10.46265/genresj.EMOR6509>

681 Zheng, C., Amadeu, R.R., Munoz, P.R., & Endelman, J.B. (2021). Haplotype reconstruction in
682 connected tetraploid F1 populations. *Genetics*, 219. <https://doi.org/10.1093/genetics/iyab106>

683 Zych, K., Gort, G., Maliepaard, C.A., Jansen, R.C., & Voorrips, R.E. (2019). FitTetra 2.0 -
684 Improved genotype calling for tetraploids with multiple population and parental data
685 support. *BMC Bioinformatics*, 20. <https://doi.org/10.1186/s12859-019-2703-y>

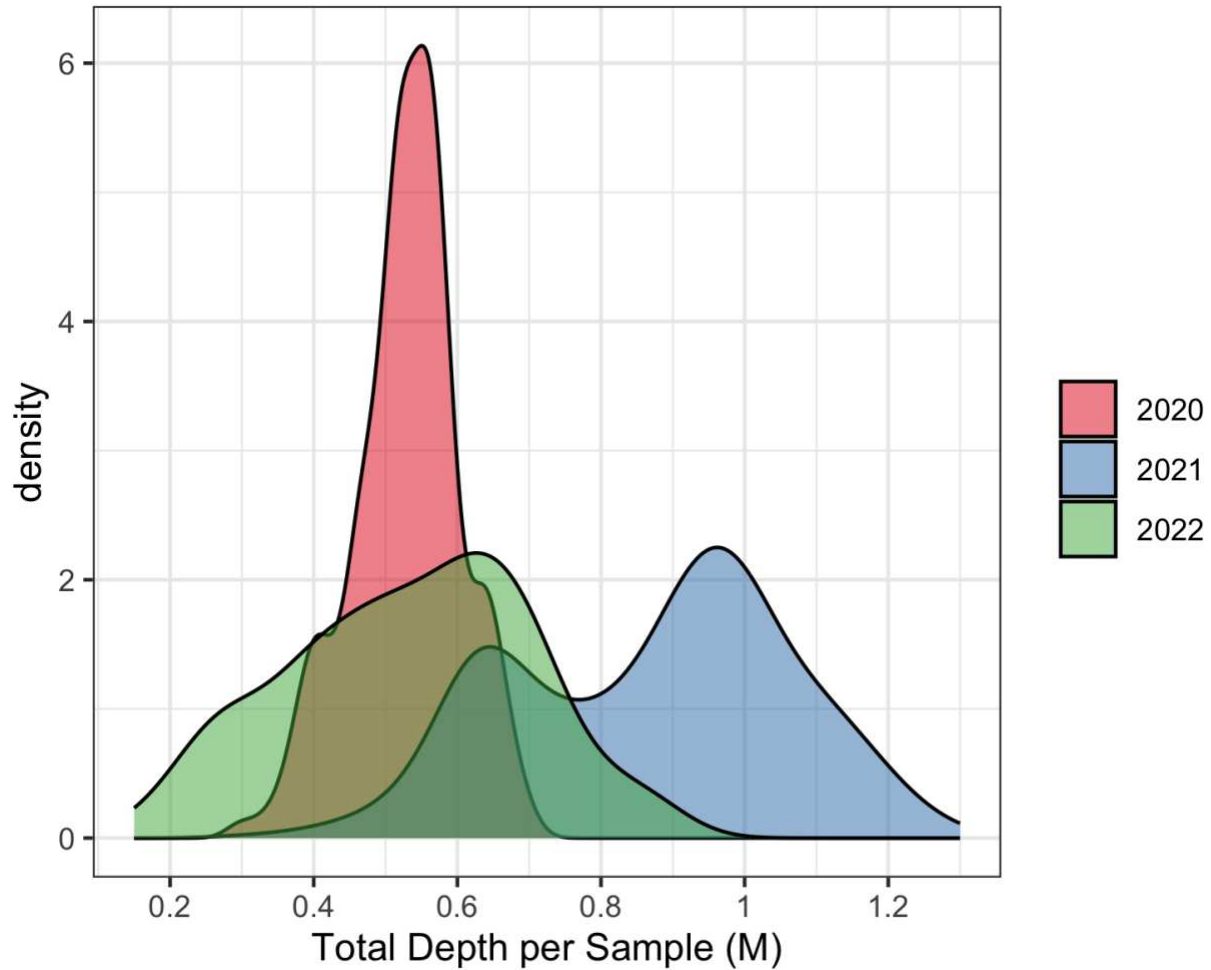


Figure 1. Total depth per sample, in million (M) read counts, for three submissions of potato V1 DArTag.

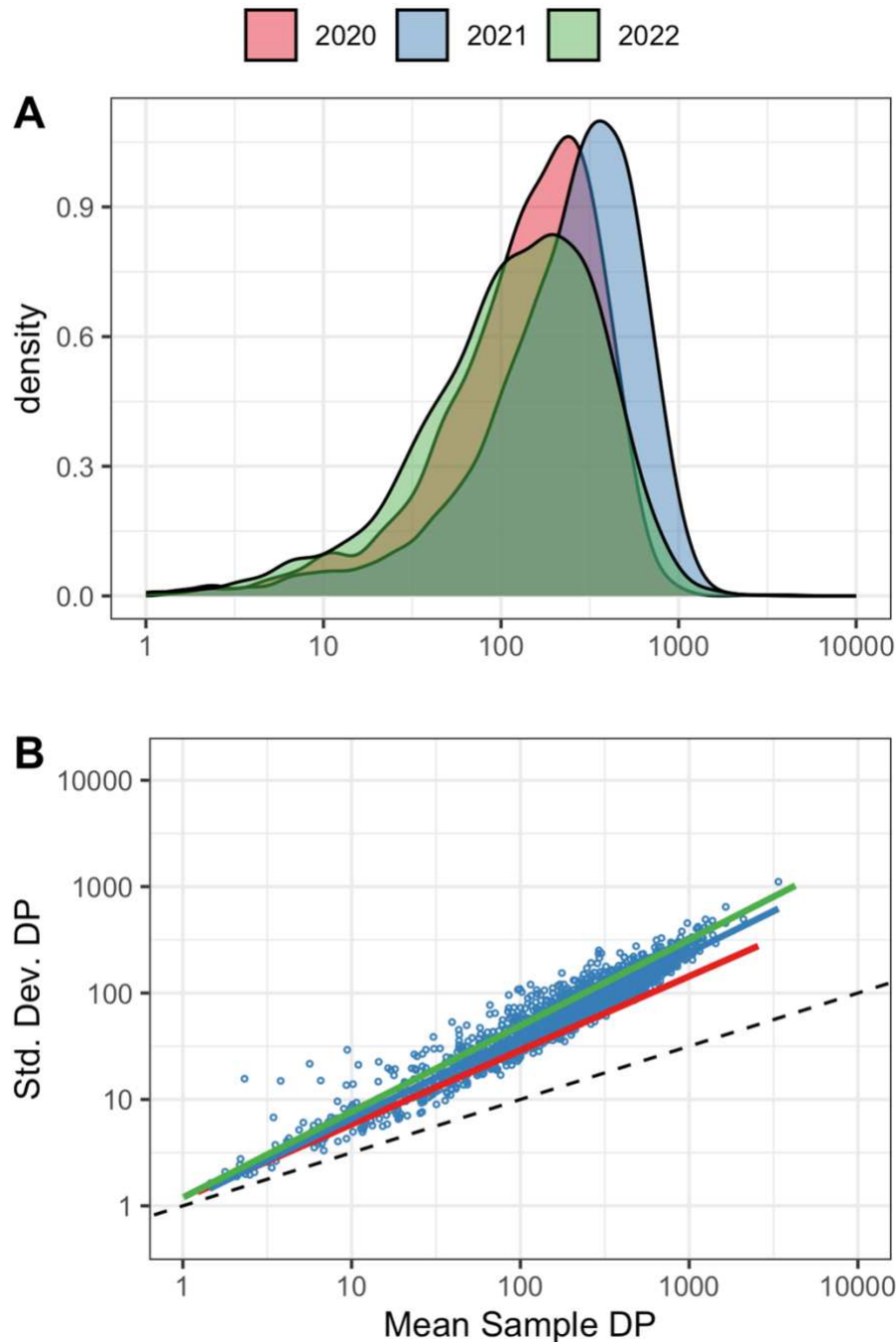


Figure 2. (A) Distribution of the mean sample depth (DP) for V1 DArTag markers. (B) Log-log plot of the relationship between the standard deviation and mean for sample DP. Individual marker points are shown only for 2021 to maintain legibility. Combining the data across years, the overall regression line (not shown) has slope 0.79 (SE 0.00) and $R^2 = 0.99$.

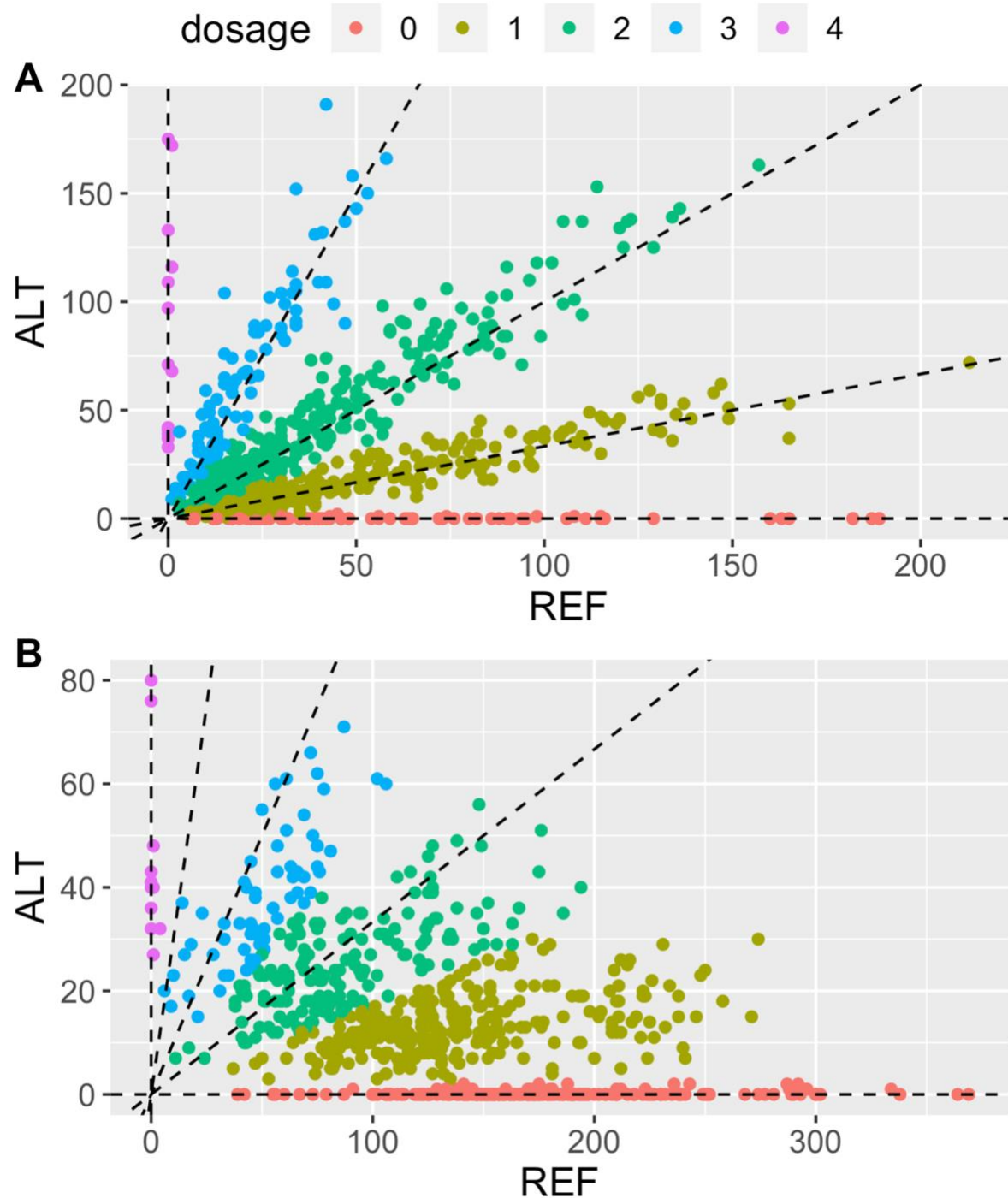


Figure 3. Examples of DArTag markers without (A) vs. with (B) allelic bias. Dashed lines correspond to possible tetraploid allele ratios when there is no allelic bias (1:0, 3:1, 1:1, 1:3, 0:1). (A) solcap_snp_c2_36615 with bias = -0.2. (B) PotVar0072076 with bias = 1.8.

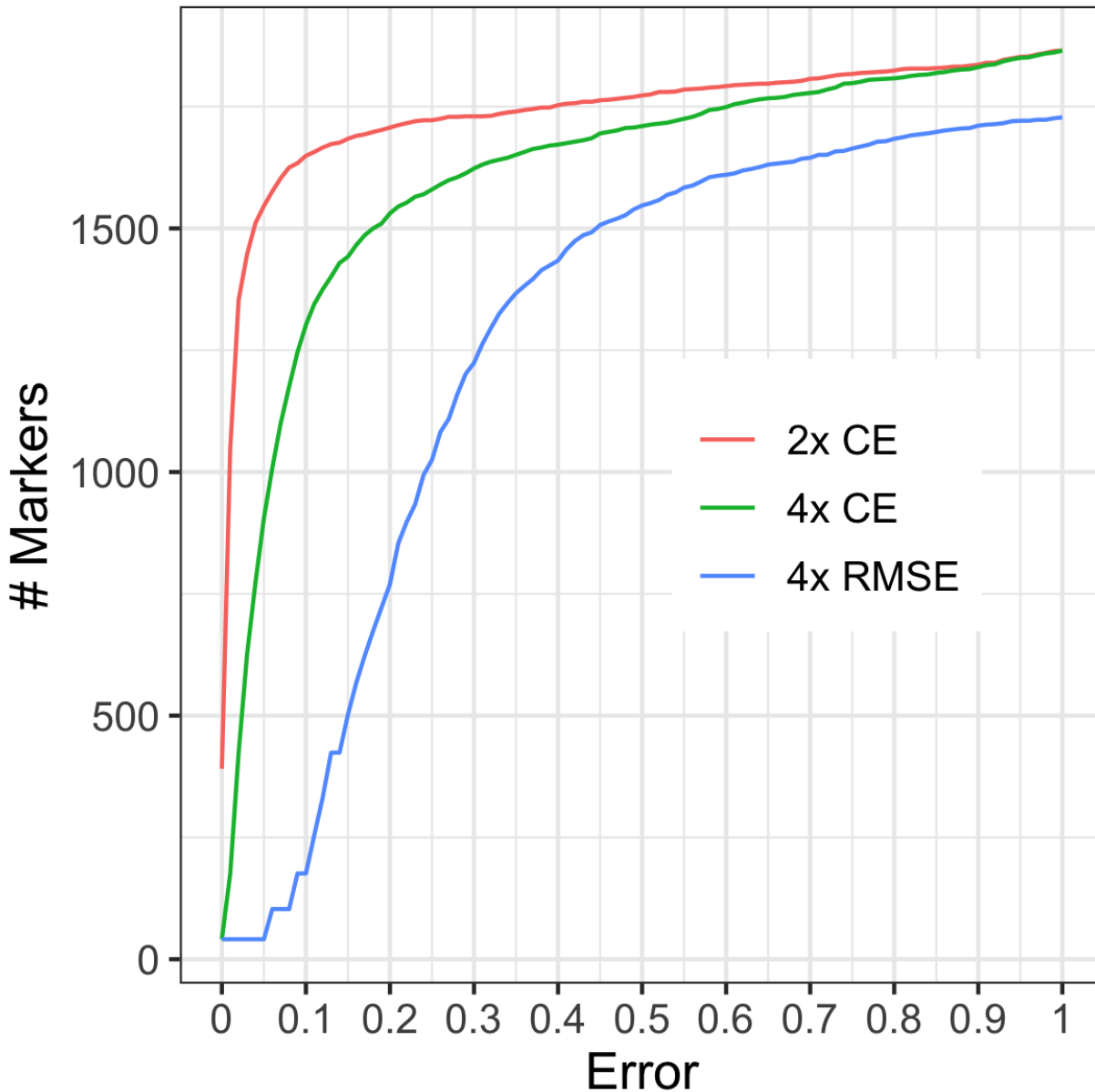


Figure 4. Empirical cumulative distribution for the error between the V1 DArTag and SNP array on 1865 common markers. CE = classification error. RMSE = root-mean-squared-error. 2x = pseudo-diploid genotypes. 4x = tetraploid genotypes.

		Corrected				
		0	1	2	3	4
Original	0	24				
	1		60	2		
	2		23	7		
	3			5	0	
	4			2		0
Original		Corrected				
		0	1	2	3	4
		0	23			
		1		61	3	
		2		10	21	3
		3			2	0
		4				0

Figure 5. Original vs. corrected genotypes for the trait markers Ryadg_chr11_2499502 and H1_chr05_52349069. The original genotypes were based on R/updog with a “norm” prior and then corrected based on linkage analysis.

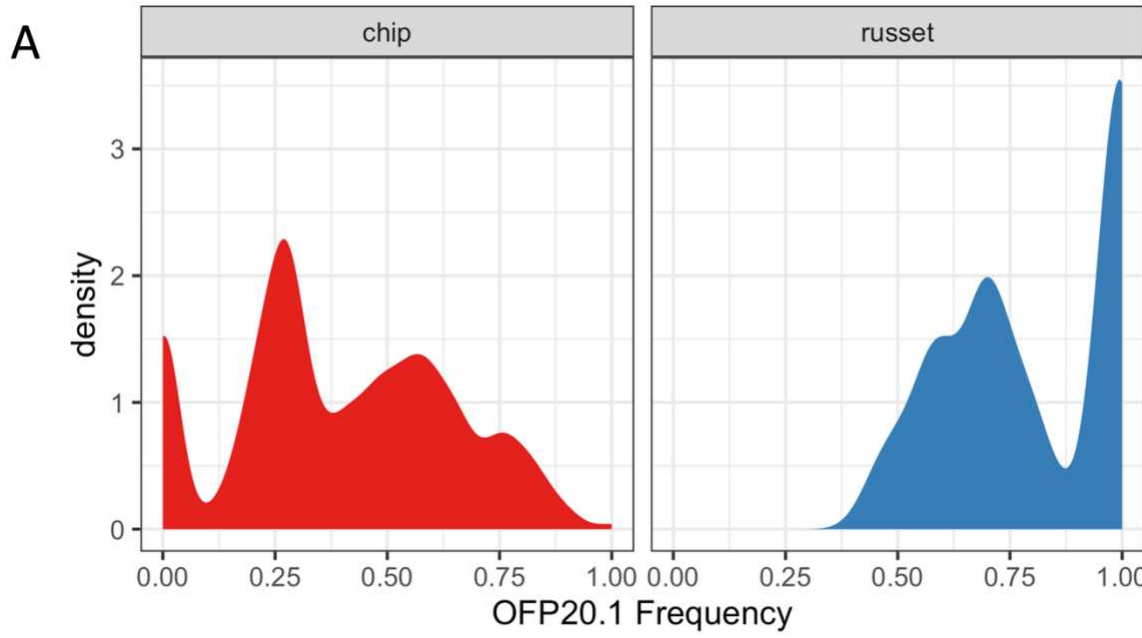
A

CDF1.4_chr05_4488021 Ref	GAAGCGGCTAAAGCTCTATATGGTCAACACTAG-----GTAT
CDF1.4_chr05_4488021 Other1	GAAGCGGCTAAAGCTCTATATGGTC <ins>C</ins> ACACTAG-----GTAT
CDF1.4_chr05_4488021 Other2	GAT <ins>G</ins> GGCTAAAGCTCTATATGGTCAACACTAG-----GTAT
CDF1.4_chr05_4488021 Alt	GAAGCGGCTAAAGCTCTATATGGTCAACACTAG <ins>GTATCCC</ins> GTAT
CDF1.4_chr05_4488021 Other3	GAAGCGGCTAAAGCTCTATATGGTCAACACTAG <ins>TCACTA</ins> GTAT

B

	CDF1.1 Count	CDF1.2 Count	CDF1.4 Count	CDF1 Genotype
Atlantic	23	0	34	1/3/4/4
W13069-5-DH088	87	0	64	1/4
W14NYQ29-5-DH024	77	0	0	1/3
RioColorado-DH005	122	81	0	1/2
W9968-5-DH151	0	18	0	2/3
W2x001-22-45	0	0	0	3/3

Figure 6. (A) Multiple sequence alignment of the DArTag haplotypes discovered for trait marker CDF1.4_chr05_448021. Haplotypes Ref, Other1, Other2 are CDF1.1 alleles, while Alt is CDF1.4 and Other3 is CDF1.2. (B) Haplotype read counts for samples with known CDF1 genotype.



B

	OFP20 Genotype	AF Allele 1	AF Allele 8	AD Alleles 2,3+7
CO99076-6R-DH002	1/1	1.00	0.00	0,0
W14NYQ29-5-DH024	3/3	0.00	0.00	0,240
W14NYQ9-2-DH137	1/3	0.49	0.00	0,115
W8890-1R-DH002	1/7	0.64	0.00	0,70
W9968-5-DH084	1/8	0.44	0.60	0,1

Figure 7. (A) Distribution of sample allele frequencies for OFP20.1 in round chip (N=300) vs. long russet (N=21) germplasm. (B) Comparison of known OFP20 genotypes with V2 DArT markers. Allele frequency (AF) of OFP20.1 was approximated by ALT frequency at marker OFP20_M6_CDS_994. AF of OFP20.8 was approximated by REF frequency at marker OFP20_M6_CDS_24. Allele depth (AD) at OFP20_M6_CDS_171 was used to distinguish allele 2 (ALT) from alleles 3 and 7 (REF).

Supplemental Figures and Tables

Endelman *et al.* Targeted genotyping-by-sequencing of potato and software for imputation.

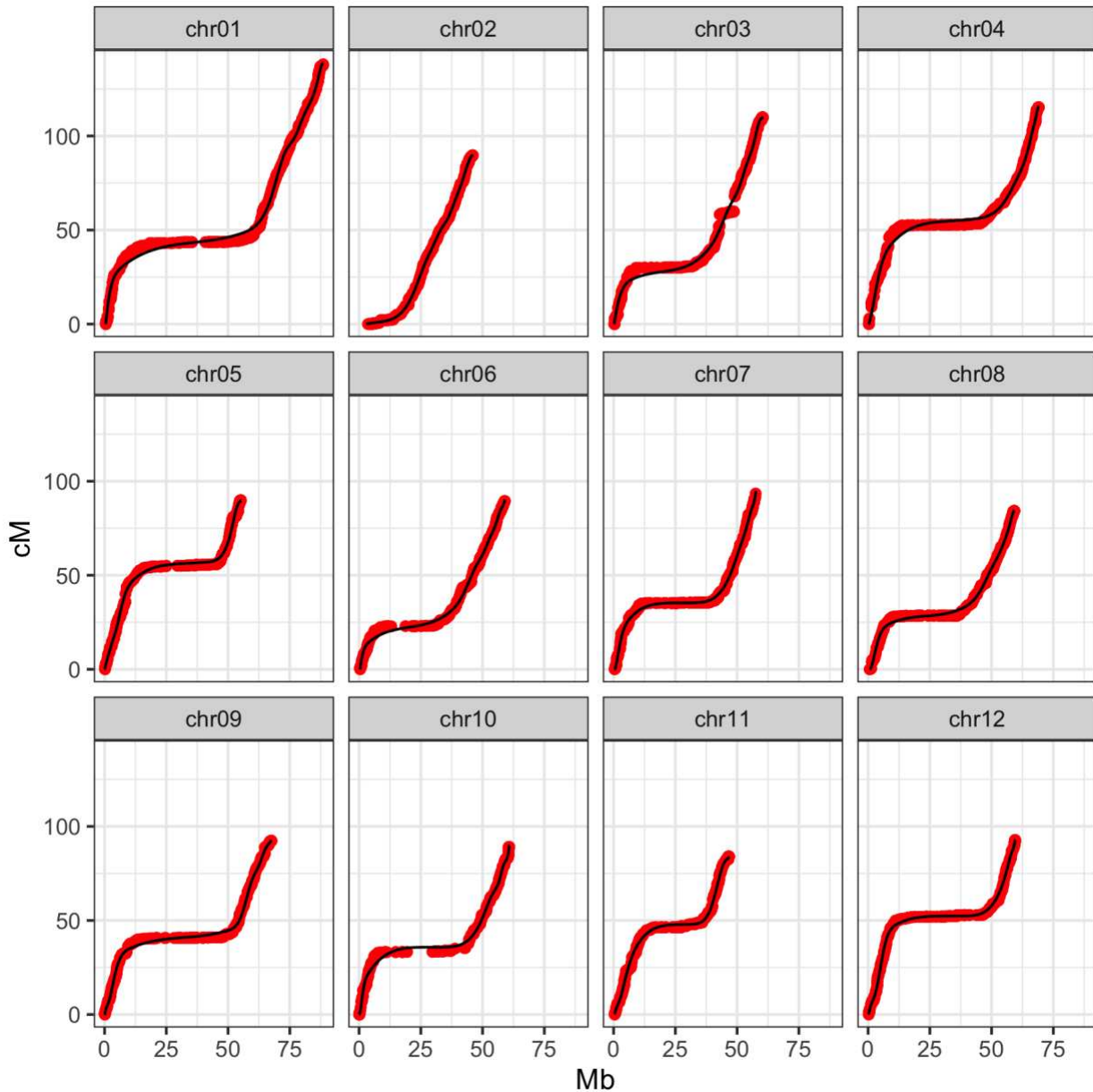


Figure S1. Marey Map of the potato genome. Horizontal axis is the DMv6.1 reference genome position (Pham et al., 2020).

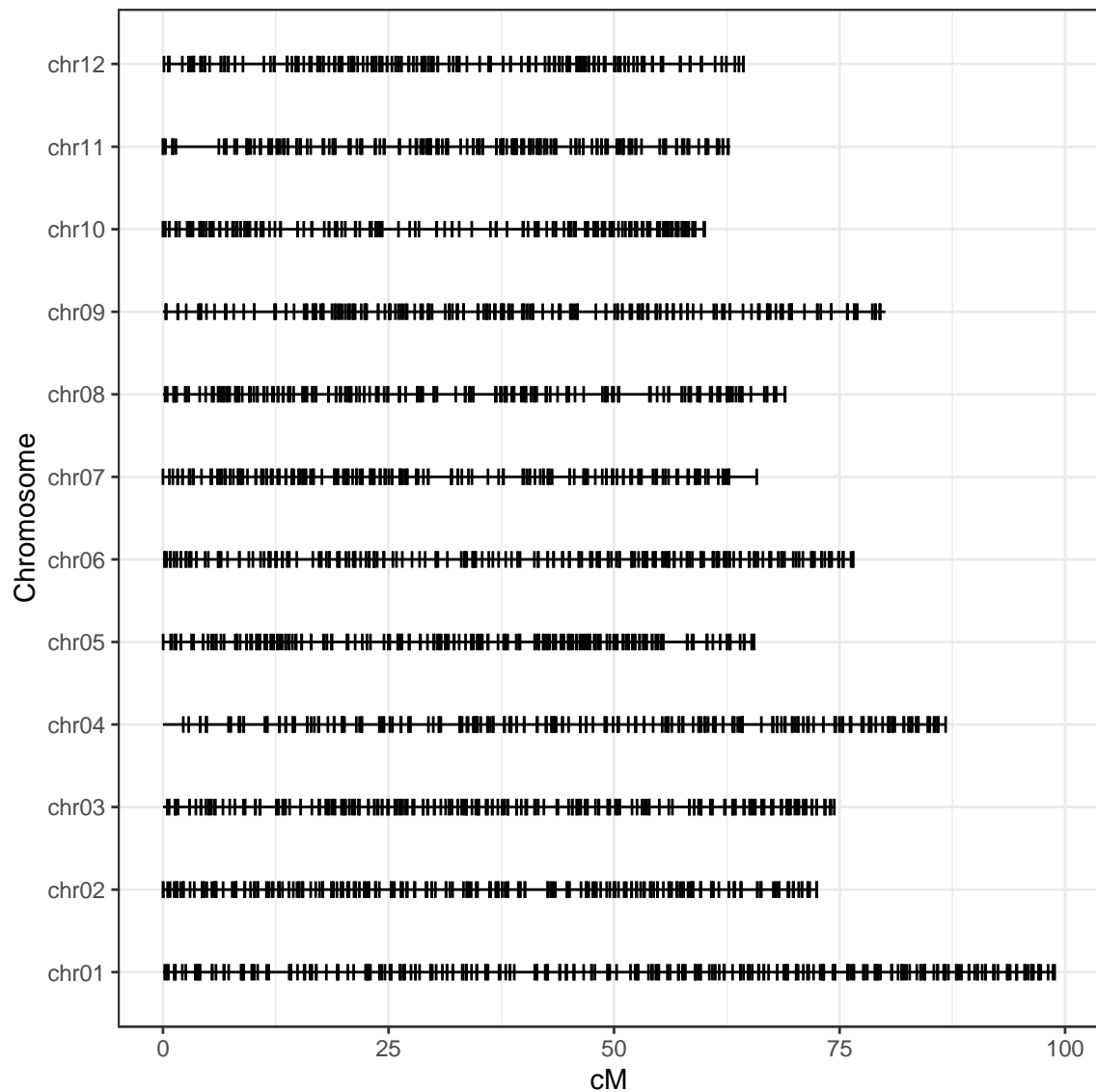


Figure S2. Distribution of the 2501 genomic markers for V1 DArTag.

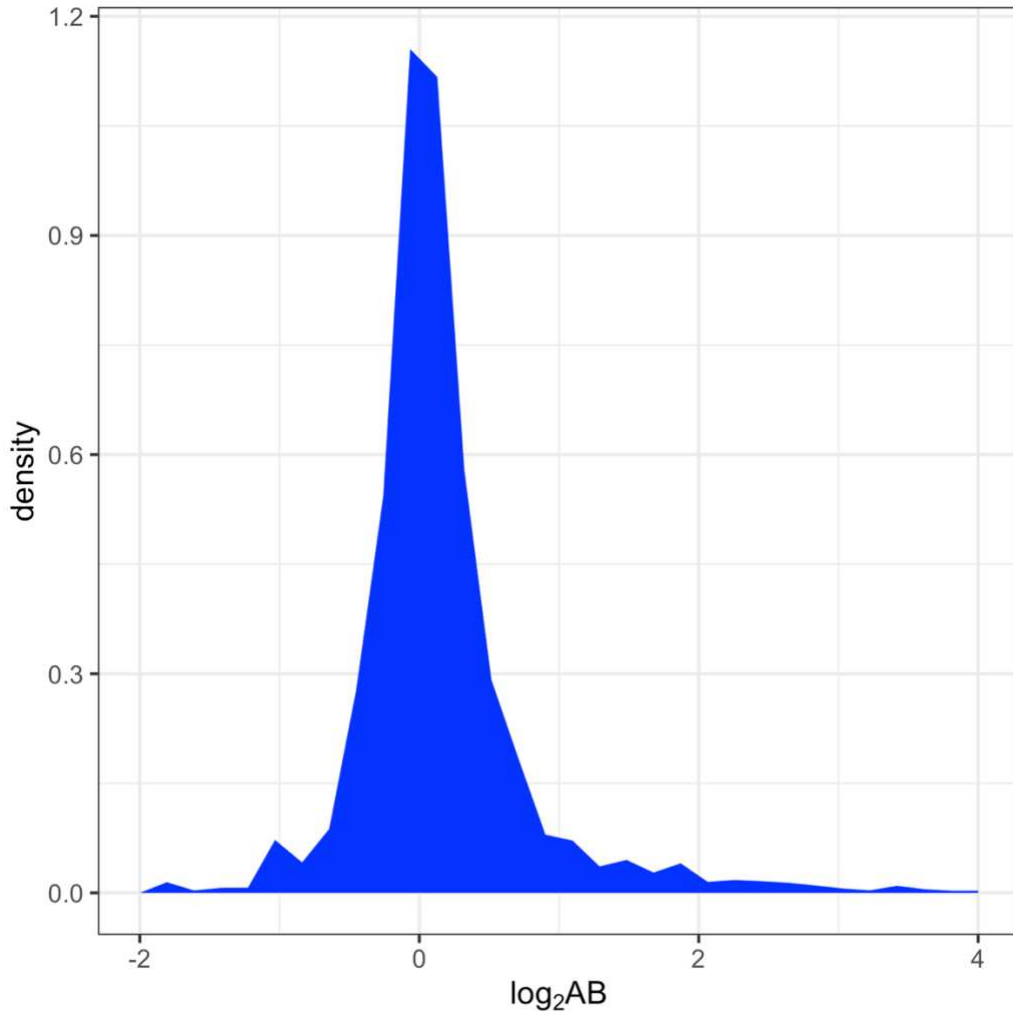
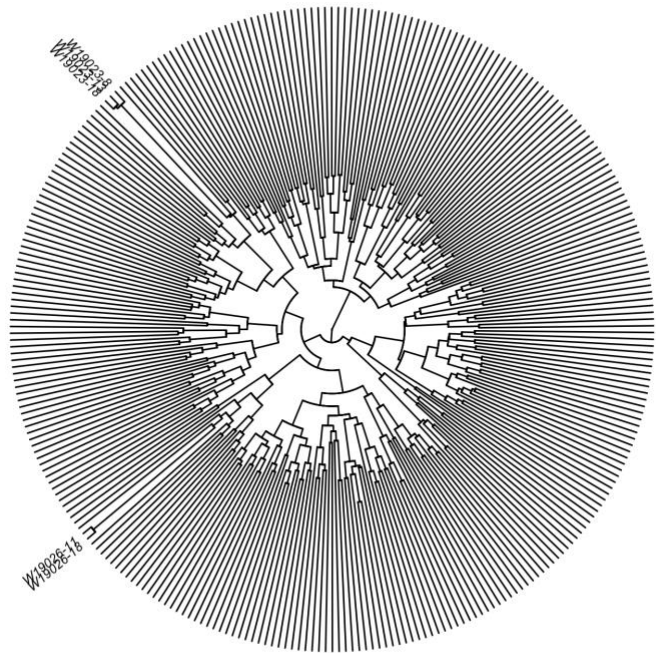


Figure S3. Distribution of allele bias (AB) estimates, where AB=1 indicates no bias, and values greater than 1 indicate bias toward the REF allele

SNP array



GBS

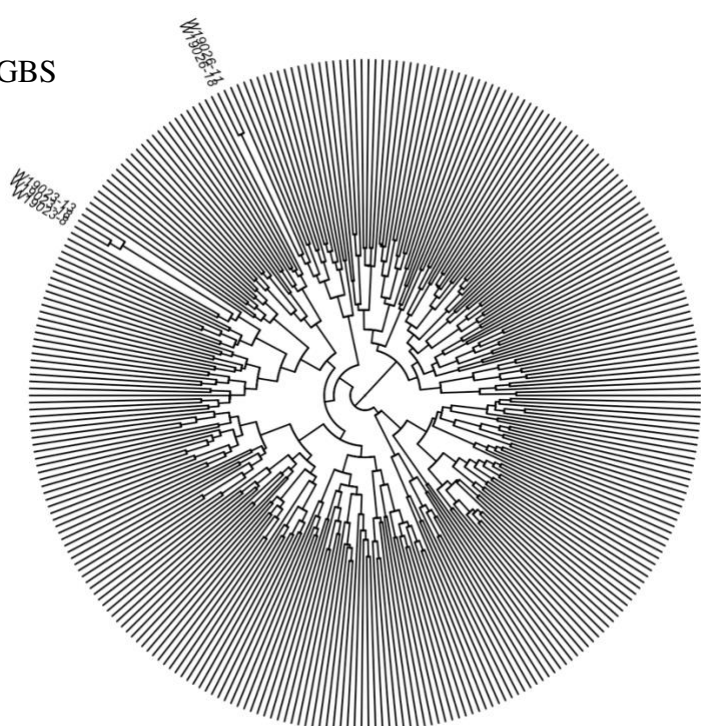


Figure S4. Hierarchical clustering based on SNP array (top) or GBS (bottom) data. Both platforms identified two groups of genetically identical clones, one pair and one threesome, originating from the same F1 populations

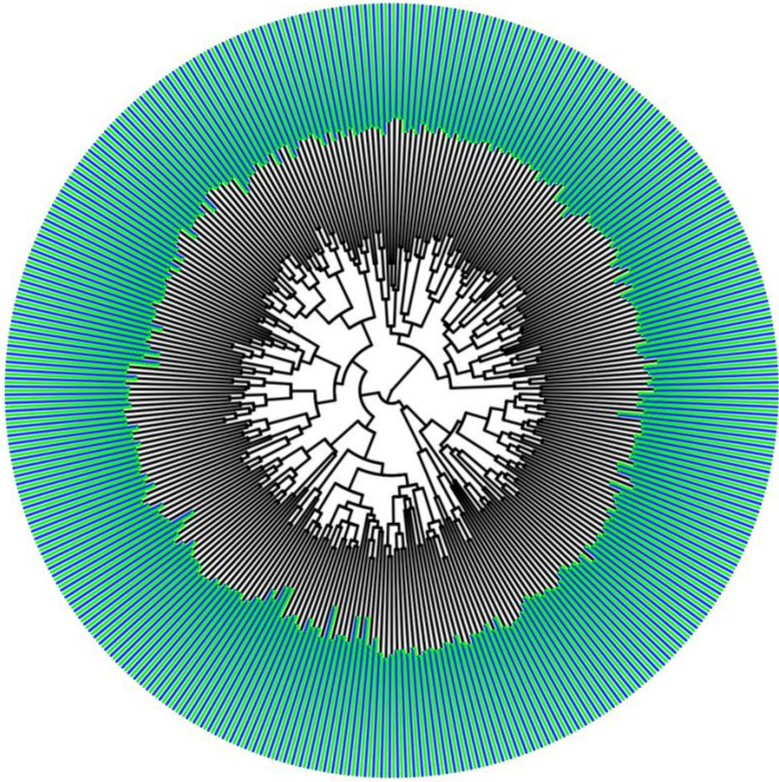


Figure S5. Joint clustering of SNP array (blue) and GBS (green) samples. The two marker profiles for every clone were paired.

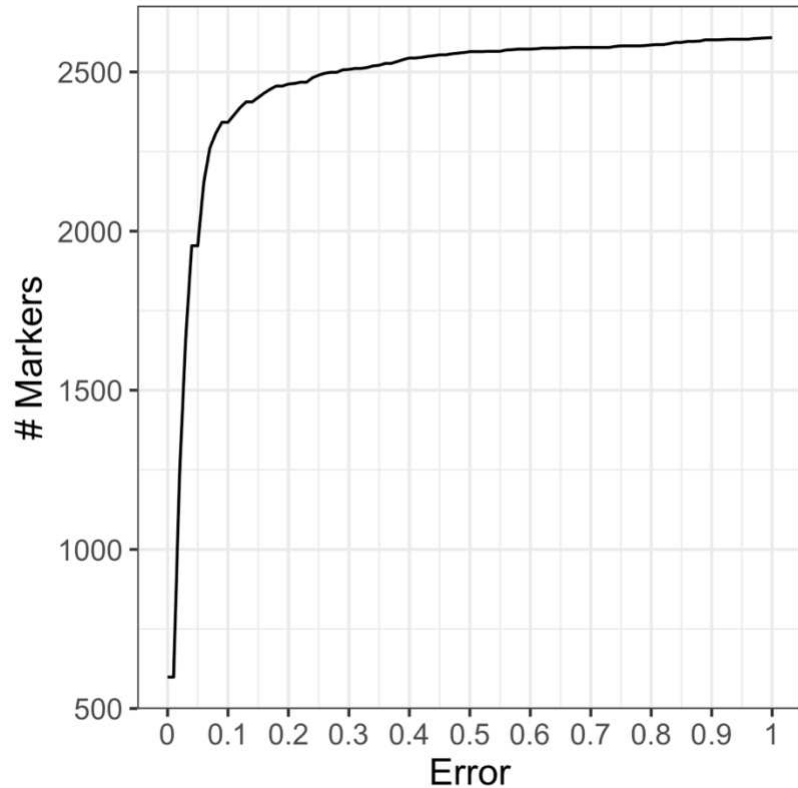


Figure S6. Empirical cumulative distribution for 2x classification error for 2608 common markers between the V4 SNP array and V2 DArTag.

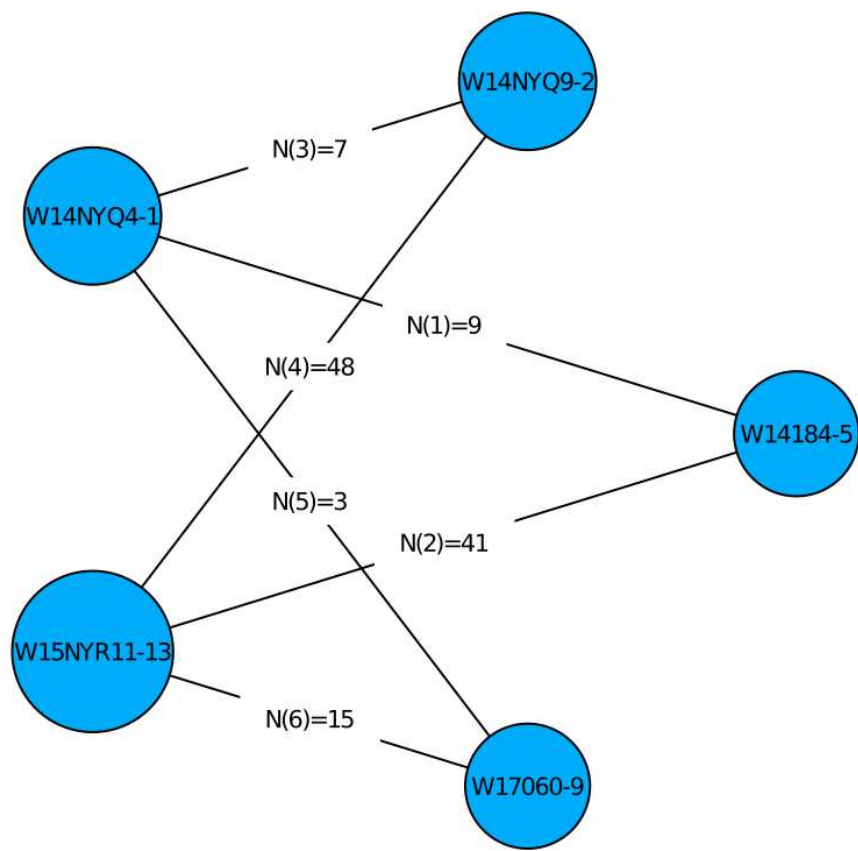


Figure S7. Five-parent partial diallel. Graphical output from PolyOrigin shows the number of progeny per biparental F1 population.

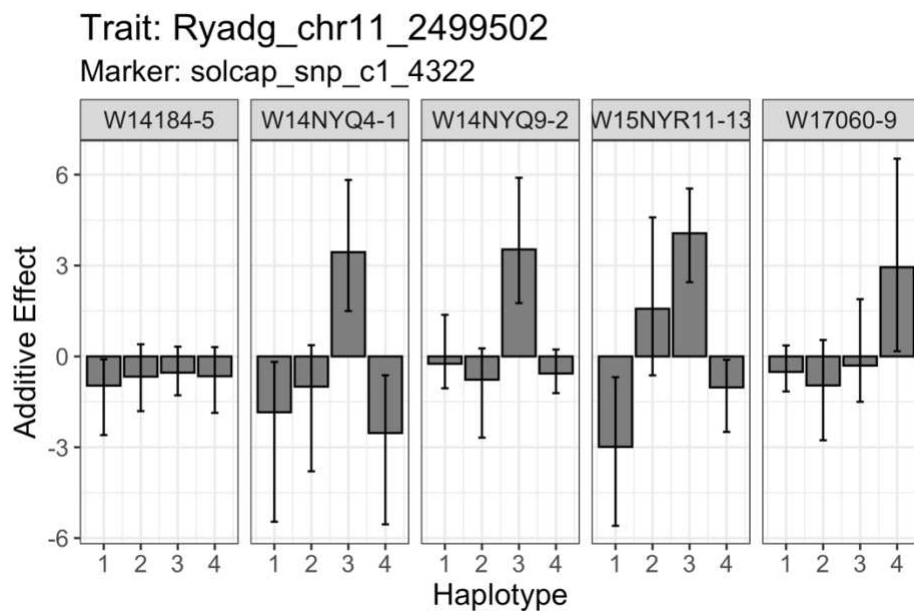
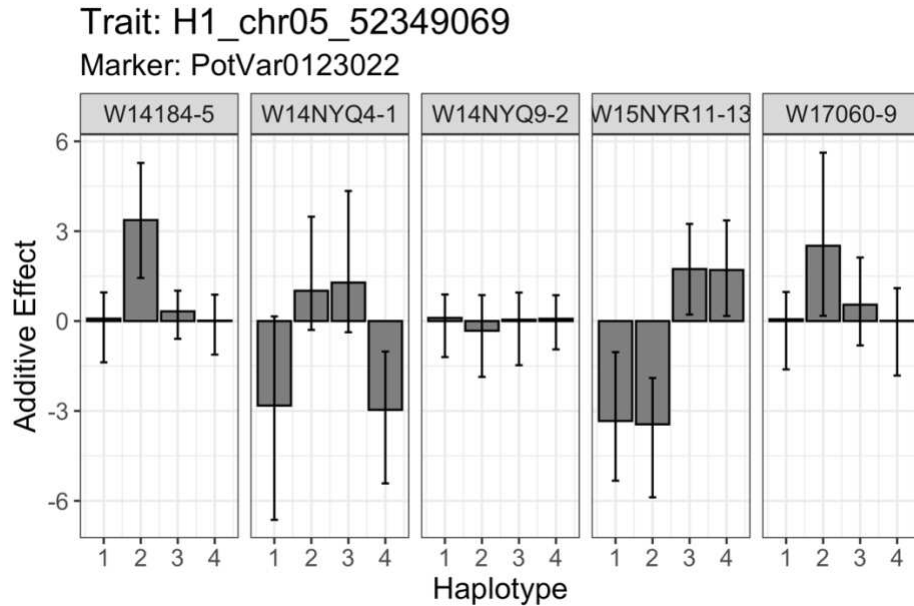


Figure S8. Additive effect estimates for parental haplotypes in the five-parent partial diallel. Positive values indicate presence of the R gene. From left to right, the result indicates the parental dosage of Ryadg is 0, 1, 1, 2, 1, and for H1 the parental dosage is 1, 2, 0, 2, 1. Parents W14NYQ9-2 and W15NYR11-13 were included in the V2 DArTag submission, and their genotype calls agree with these predictions (FileS3).

Table S1. Comparison of KASP and V1 DArTag markers targeting *Ry_{adg}* (snpST00073).

	Absent	Present
Absent	7	1
Present	1	84

Table S2. Positive samples for marker Rysto_chr12_2352742 in V2 DArTag.

id	mother	father
W17079-16rus	Payette Russet	AW07791-2rus
W17081-2rus	Payette Russet	W9742-3rus
A12304-1sto	A96953-13sto	Clearwater Russet
W6511-1R	Kankan	W2275-9R

Table S2. Results for marker Sli_chr12_2372490 in V2 DArTag.

id	ALT dosage
W9968-5-DH027	0
CO99076-6R-DH002	0
CO99076-6R-DH033	0
W14NYQ29-5-DH024	0
W14NYQ9-2-DH119	0
W14NYQ9-2-DH132	0
W8890-1R-DH003	0
W9968-5-DH084	0
W9968-5-DH022	0
W13069-5-DH088	0
RioColorado-DH003	0
W9968-5-DH151	0
W12078-76-DH352	0
W12078-76-DH099	0
W13058-4-DH002	0
W14NYQ9-2-DH137	0
W14NYQ9-2-DH146	0
RioColorado-DH005	1
W15263-50R-DH001	1
W15263-50R-DH011	1
W8890-1R-DH002	1
W9426-3R-DH005	1
W9426-3R-DH037	1
W2x150-24	1
W2x113-3	1
W2x001-22-45	2
W2x082-(14/20)-13	2
W2x082-(14/20)-13-2	2